2022

SIMULATING GROUNDWATER POLLUTANT TRANSPORT FOR REMEDIATION DESIGN, ANTRIM COUNTY, MICHIGAN

Abilynn Raetz
Michigan Technological University, aeraetz@mtu.edu

SIMULATING GROUNDWATER POLLUTANT TRANSPORT FOR REMEDIATION DESIGN, ANTRIM COUNTY, MICHIGAN

By

Abilynn E. Raetz

A REPORT

Submitted in partial fulfillment of the requirements for the degree of

MASTER OF SCIENCE

In Geological Engineering

MICHIGAN TECHNOLOGICAL UNIVERSITY

2022

This report has been approved in partial fulfillment of the requirements for the Degree of MASTER OF SCIENCE in Geological Engineering.

Department of Geological and Mining Engineering and Sciences

Report Advisor:	*Dr. John S. Gierke, PE*
Committee Member:	*Dr. Melanie Kueber Watkins, PE*
Committee Member:	*Dr. Nathan Manser, PE*
Department Chair:	*Dr. Aleksey Smirnov*

Table of Contents

List of Figures

List of Tables

Acknowledgements

Firstly, I would like to acknowledge the support and data provided by Global Remediation Technologies, Inc. This project utilizes data gathered and analyzed by GRT. I would like to thank Richard Raetz and Erin Schneider for walking me through different aspects of their ongoing remediation efforts in Torch Lake, Michigan.

I want to thank my advisor, Dr. John S. Gierke, for the support, guidance, time, and jokes shared throughout this project. I appreciate all of the advice you have given me, from mathematical modeling to blueberry pie recipes.

Thank you to my committee members, Dr. Melanie Kueber Watkins and Dr. Nathan Manser, whose courses helped shape my project idea and career goals. A debt of gratitude is owed for taking time out of their busy schedules to serve on my committee.

Thanks to Brittany Buschell, Jenna Laird, and Luke Bowman for their help and support in keeping the GMES department running smoothly.

Thank you to my parents, Linda and Richard Raetz, for supporting my education and always sharing encouragement and advice.

Thank you to Reggie and Kyle Hrubecky for the support and patience you both have shown through my schooling and always being ready to take a break with me.

To all of my friends in Houghton, thank you for the laughs, games, bike rides, and more. You are what makes the Keweenaw so unique.

List of Abbreviations

ATSDR	Agency for Toxic Substances and Disease Registry
ASTER	Advanced Spaceborne Thermal Emission and Reflection Radiometer
DOT	Department of Transport
DNR	Department of Natural Resources
EGLE	Environment, Great Lakes, and Energy (formerly known as Michigan's Department of Environmental Quality)
EMB	Enhanced Microbial Bioremediation
ESRI	Environmental Systems Research Institute
GIS	Geographic Information Systems
GRT	Global Remediation Technologies, Inc
GMS	Groundwater Modeling System
LNAPL	Light non-aqueous phase liquids, such as diesel
MDEQ	Michigan’s Department of Environmental Quality
NASA	National Aeronautics and Space Administration
NOAA	National Oceanic and Atmospheric Administration
NPDWR	National Primary Drinking Water Regulations
NWS	National Weather Service
PEST	Parameter Estimation
PVC	Polyvinyl chloride
US EPA	United States Environmental Protection Agency
USACE	United States Army Corp of Engineers
USGS	United States Geological Survey

Abstract

Located in Antrim County, Michigan between the coasts of Torch Lake and Lake Michigan is a hydrocarbon plume that has impacted surrounding residential wells. The plume is comprised of benzene, toluene, ethylbenzene, and xylenes (BTEX) and primarily resides in the shallowest groundwater aquifer. The plume is suspected of having originated from an underground storage container that was removed in 1979. A conceptual model was developed for the site, comprising of a simplified hydrogeological model. Groundwater modeling was performed using Aquaveo's groundwater modeling software (GMS). PEST parameter calibration was performed on the hydraulic conductivity and recharge values using data from surrounding wells. These values were then used to create a reasonable steady-state regional flow model. The groundwater flow code MODFLOW was used to simulate the steady-state flow model. The use of MT3DMS simulated the fate and transport of the BTEX to inform remediation design. The model simulated natural attenuation, air injection, and enhanced microbial bioremediation (EMB) to project aquifer behavior and contaminant degradation for each remediation technique. Results showed that EMB degraded the plume the lowest, to 2 mg/L after 91 days. While modeling can be a time-efficient and cost-saving technique, it should be coupled with value engineering and site investigation when designing a remediation system.

1 Introduction

Hydrocarbon contamination occurs due to aging infrastructure that supports the storage and transport of oil and gas (Li, 2017). When present in groundwater, benzene, toluene, ethylbenzene, and xylenes, commonly referred to as BTEX, can account for 90% of the petroleum plume in the soil-water complex (Mitra & Roy, 2011; Wiedemeier et al., 1996; Wilbur & Bosch, 2004). These organic compounds can lead to anoxic conditions in the environment, contaminate drinking water aquifers, and travel long distances without proper remediation (ATSDR, 2021).

Due to the costly nature of remediation, fate and transport modeling can help inform remediation design. This project focuses on modeling the effect of natural attenuation, air injection, and enhanced microbial bioremediation (EMB) on a BTEX plume in Antrim County, Michigan. Standard biologically focused remediation techniques for BTEX are natural attenuation, air injection, and EMB (Bruce et al., 2010; Lu et al., 1999; Ritman et al., 2000; Wiedemeier et al., 1996). Natural attenuation utilizes the microbial community already present in the environment to reduce the BTEX constituents to CO_2 and water. This technique requires monitoring over a long period (Ritman et al., 2000). Air injection adds dissolved oxygen *in-situ* to help promote microbial activity (Landmeyer & Bradley, 2003; Zengguang et al., 2015). EMB, as used herein, is the *in-situ* addition of microbes and amendments (air and nutrients) that degrade BTEX constituents, similar to natural attenuation but typically on a more rapid scale (El-Naas et al., 2014; Wiedemeier et al., 1996). Either aerobic or anaerobic microorganisms can be utilized depending on the target contamination and aquifer conditions.

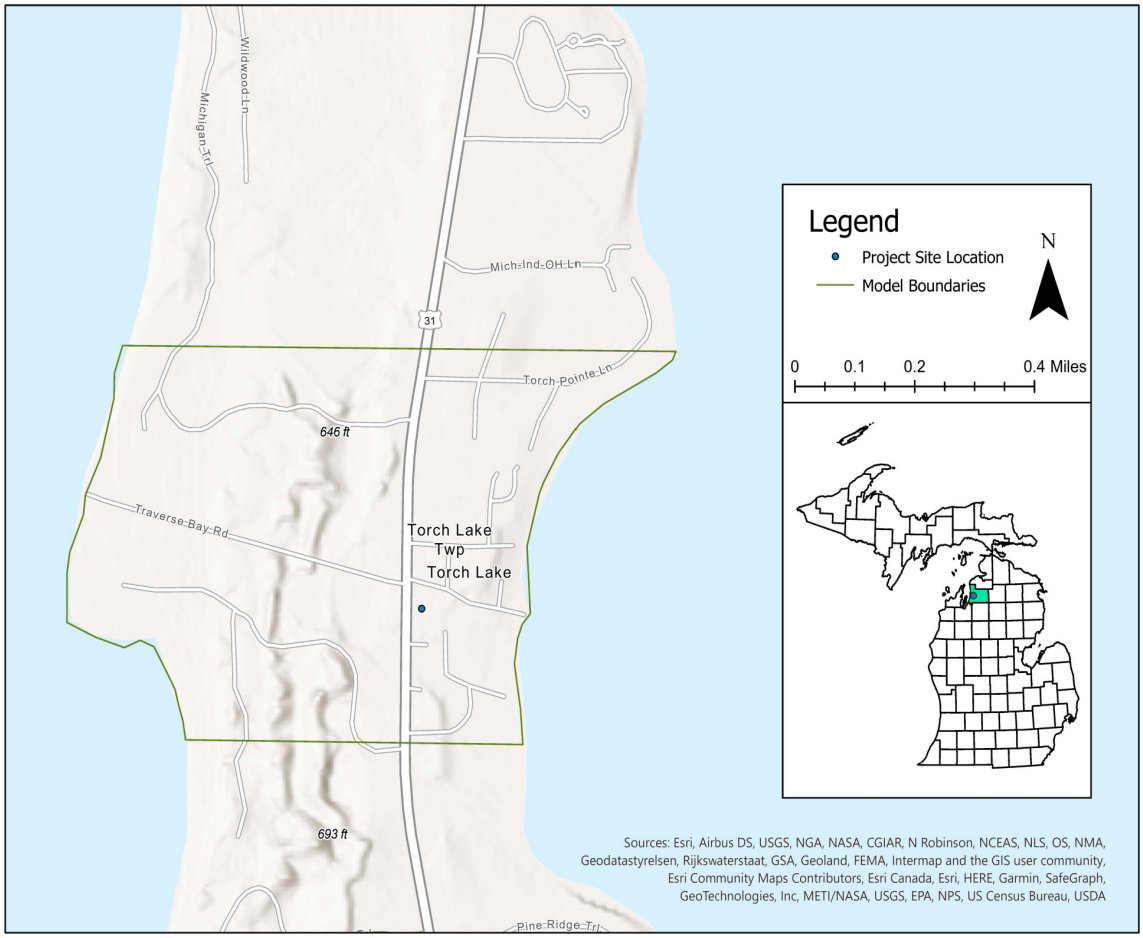

Figure 1.1: Study site location denoted by point in Torch Lake Township, Antrim County, Michigan. Reference data, such as roads and counties are shown.

2 Project Site Background

The project is located in Torch Lake Township in Antrim County, Michigan, where the Torch Lake Standard, a gas station, was previously in operation until 1979. The project site has residential properties adjoining the south, east, and west boundaries. A seasonal ice cream shop (31 Scoops) operates along the northern border, and the William K. Good Day Park is further to the East along the shore of Torch Lake. Torch Lake Standard Gas is no longer in operation, and the parcel is presently used as a residence, composed of a home and storage unit on the premises (Antrim County Michigan, 2017).

2.1 Remediation Site History

Between 1978 and 1992, three residential wells in Torch Lake Township were impacted by petroleum constituents. The state replaced these wells with deeper wells below the impacted aquifer. The suspected source of the hydrocarbon constituents was an underground storage container for the Torch Lake Standard gas station, which was removed concurrently with the closure of the station in 1979 (GRT, 2019). One commercial and three residential properties surround the project (Antrim County Michigan, 2017).

The state of Michigan provided funding from 1999 to 2003 for site investigation to characterize the extent of pollution. The initial findings showed hydrocarbon constituents that exceeded regulatory levels per Part 201 of the Natural Resources and Environmental Protection Act, P.A, 451 of 1994, as amended (Part 213) in the soils and shallow groundwater aquifer (EGLE, 2020a; GRT, 2019; Haynes, 2011). In 2010, a state contractor attempted to remediate the plume source using vacuum enhanced product recovery. The contractor's efforts removed 3,486 gallons of water/plume mixture and an estimated 25.7 pounds of contaminant mass in the vapor phase. However, enough contaminant remained above regulatory levels.

In 2012, laser-induced fluorescence was utilized on-site to identify areas of LNAPL at the water table surface. In June 2013, an air-sparge/soil extraction system was installed and modified for site-specific use to begin the following year. The system operated until August 2015.

In 2015, Global Remediation Technologies, Inc. (GRT) was hired as a consulting firm by Environmental, Great Lakes, and Energy (EGLE) to perform a site investigation to determine a remediation strategy for the site. Their site investigation included analyzing soil borings, installing monitoring wells, assessing current septic systems, installing soil vapor pins (sampling devices), and monitoring the area to evaluate the groundwater plume concentrations. The remedial investigation concluded in 2019, and GRT suggested running a focused feasibility study for a bioremediation design, including a tracer study and pump tests (GRT, 2019).

2.2 Geology

The bedrock underlying Antrim County is the relatively impermeable shale, ranging in depths from 200 to 800 feet below ground surface. Antrim Shale is composed primarily of quartz, illite, and kerogen and appears gray to black. It may also contain kaolin, chlorite, and pyrite. The surface material is a mixture of sand and gravels, part of Pleistocene glacier deposits. These deposits are composed of outwash, till, and lacustrine deposits (Apple & Reeves, 2007; MDEQ, 2005). The project site has two main Quaternary land systems, dune sand and coarse lacustrine deposits, separated by a transect running north to south through the project extents as shown in Figure 2.2 (Farrand & Bell, 1998). There are 26 monitoring wells throughout the project site that have corresponding well logs taken on the day of well instillation. These well logs provide the location of the well, well instillation materials and method, and the stratigraphy of the sediment within the boring hole, as well as other applicable information. The recorded stratigraphy can be used to infer the heterogeneity of the sediment and can be used to determine aquifer properties. An example of a well log for Well ID: 05000005718 can be seen in Figure 2.1 (EGLE, 2022).

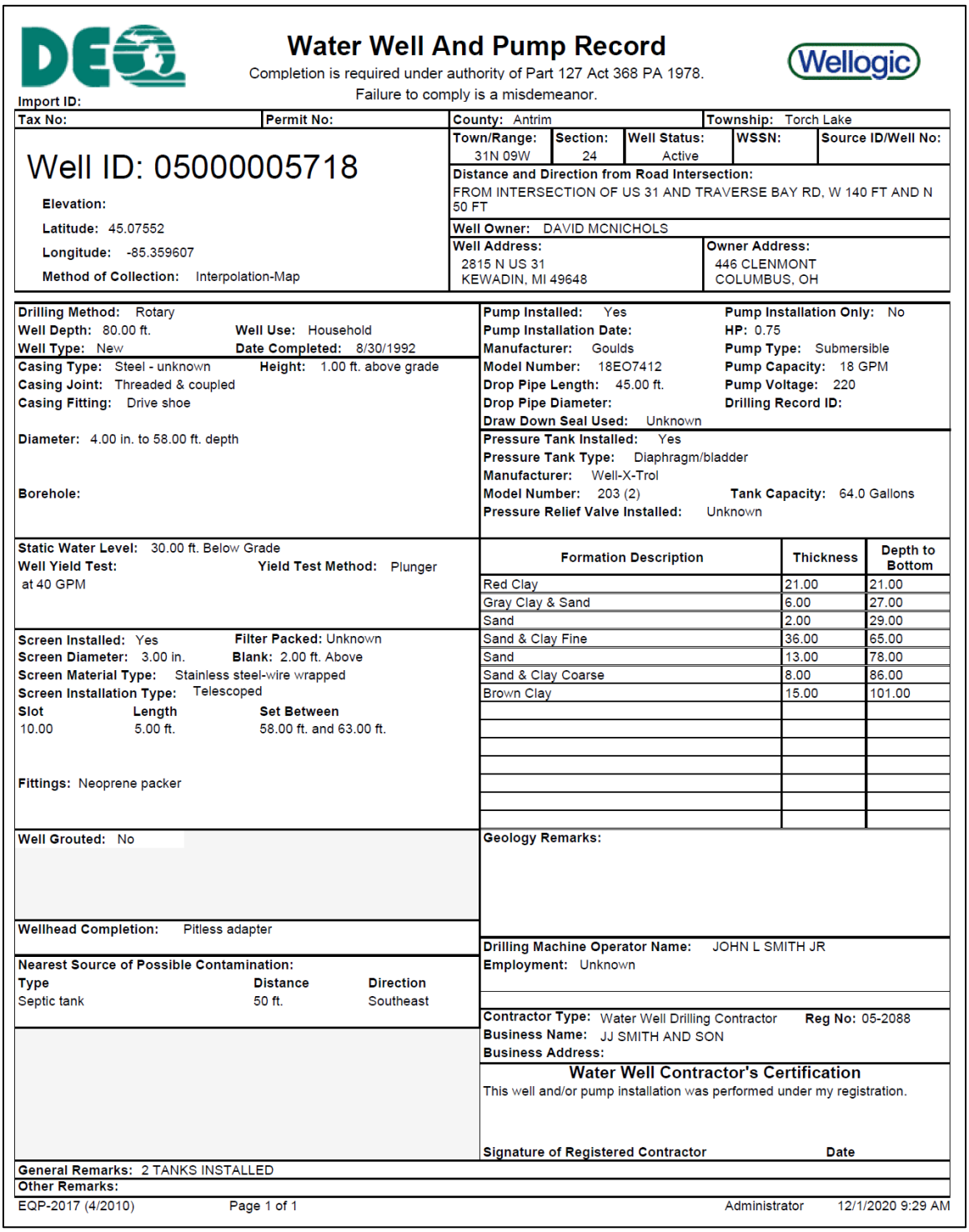

Water Well And Pump Record

Completion is required under authority of Part 127 Act 368 PA 1978.
Failure to comply is a misdemeanor.

Wellogic

Import ID:

Tax No:	Permit No:	County: Antrim			Township: Torch Lake	
		Town/Range: 31N 09W	Section: 24	Well Status: Active	WSSN:	Source ID/Well No:

Well ID: 05000005718

Elevation:
Latitude: 45.07552
Longitude: -85.359607
Method of Collection: Interpolation-Map

Distance and Direction from Road Intersection:
FROM INTERSECTION OF US 31 AND TRAVERSE BAY RD, W 140 FT AND N 50 FT

Well Owner: DAVID MCNICHOLS

Well Address:	Owner Address:
2815 N US 31 KEWADIN, MI 49648	446 CLENMONT COLUMBUS, OH

Drilling Method: Rotary
Well Depth: 80.00 ft. **Well Use:** Household
Well Type: New **Date Completed:** 8/30/1992

Casing Type: Steel - unknown **Height:** 1.00 ft. above grade
Casing Joint: Threaded & coupled
Casing Fitting: Drive shoe

Diameter: 4.00 in. to 58.00 ft. depth

Borehole:

Static Water Level: 30.00 ft. Below Grade
Well Yield Test: **Yield Test Method:** Plunger
at 40 GPM

Screen Installed: Yes **Filter Packed:** Unknown
Screen Diameter: 3.00 in. **Blank:** 2.00 ft. Above
Screen Material Type: Stainless steel-wire wrapped
Screen Installation Type: Telescoped

Slot	Length	Set Between
10.00	5.00 ft.	58.00 ft. and 63.00 ft.

Fittings: Neoprene packer

Well Grouted: No

Wellhead Completion: Pitless adapter

Nearest Source of Possible Contamination:

Type	Distance	Direction
Septic tank	50 ft.	Southeast

Pump Installed: Yes **Pump Installation Only:** No
Pump Installation Date: **HP:** 0.75
Manufacturer: Goulds **Pump Type:** Submersible
Model Number: 18EO7412 **Pump Capacity:** 18 GPM
Drop Pipe Length: 45.00 ft. **Pump Voltage:** 220
Drop Pipe Diameter: **Drilling Record ID:**
Draw Down Seal Used: Unknown

Pressure Tank Installed: Yes
Pressure Tank Type: Diaphragm/bladder
Manufacturer: Well-X-Trol
Model Number: 203 (2) **Tank Capacity:** 64.0 Gallons
Pressure Relief Valve Installed: Unknown

Formation Description	Thickness	Depth to Bottom
Red Clay	21.00	21.00
Gray Clay & Sand	6.00	27.00
Sand	2.00	29.00
Sand & Clay Fine	36.00	65.00
Sand	13.00	78.00
Sand & Clay Coarse	8.00	86.00
Brown Clay	15.00	101.00

Geology Remarks:

Drilling Machine Operator Name: JOHN L SMITH JR
Employment: Unknown

Contractor Type: Water Well Drilling Contractor **Reg No:** 05-2088
Business Name: JJ SMITH AND SON
Business Address:

Water Well Contractor's Certification
This well and/or pump installation was performed under my registration.

Signature of Registered Contractor **Date**

General Remarks: 2 TANKS INSTALLED
Other Remarks:

EQP-2017 (4/2010) Page 1 of 1 Administrator 12/1/2020 9:29 AM

Figure 2.1: Example of a Wellogic well log for Well ID: 05000005718. Data was retrieved from the GeoWebFace Mapper that is managed by EGLE (EGLE, 2022).

2.3 Hydrology

The project site is located at the boundary of two sub-watersheds (12-digit watershed boundaries, HUC12), Spencer Creek-Torch Lake watershed and the Birch Lake-Frontal Grand Traverse Bay watershed and is in the broader Michigan Basin, as shown in Figure 2.2 (EGLE, 2020b). The project site resides between two significant hydrologic features- west of Torch Lake and east of Lake Michigan, with water surface elevations of 591 feet and 574 feet, respectively[1]. No streams or rivers run through the project site.

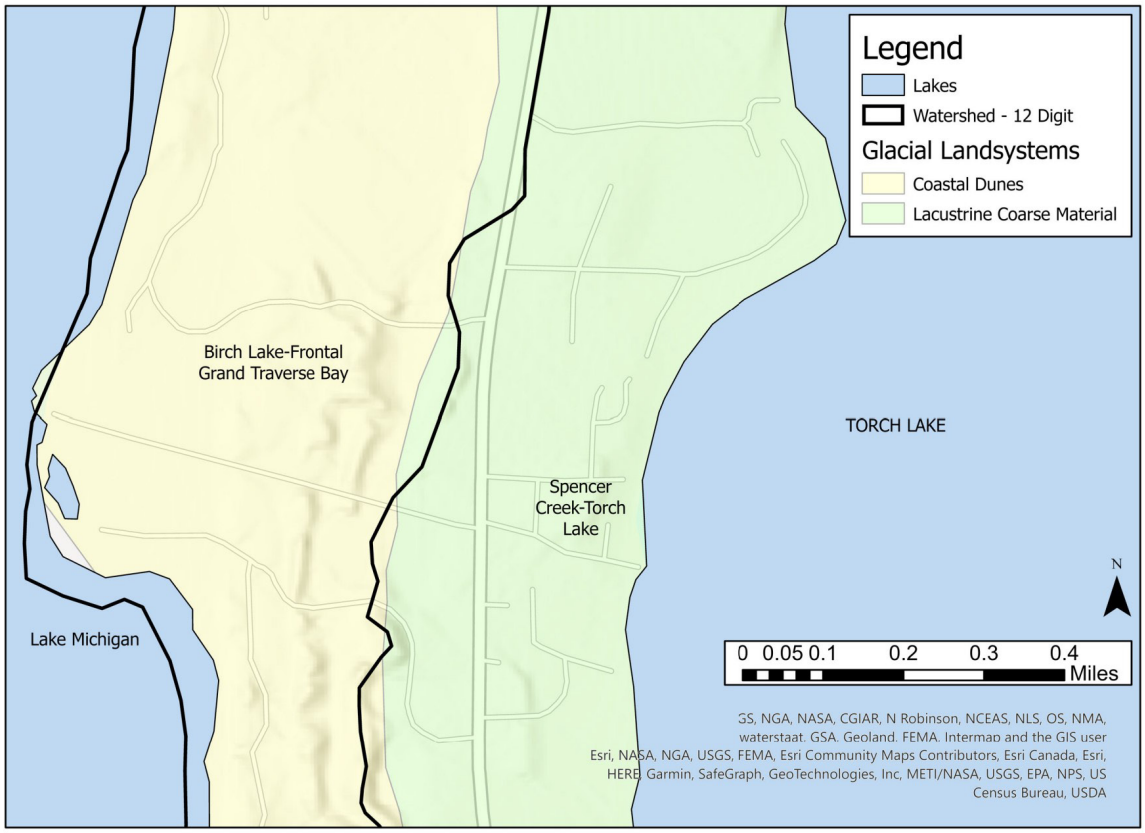

Figure 2.2: 12-digit watershed and Quaternary map of project site (EGLE 2020b; Farrand & Bell, 1998).

Three aquifers, which were termed the shallow, intermediate, and deep zones, were identified by GRT. These zones were classified using soil boring observations, subsurface geologic data, and groundwater elevation measurements by GRT (GRT, 2019). The shallow and intermediate zones can be modeled as a single unconfined aquifer due to the shallow groundwater surface slope across the flow field. The scope of this project will not include the deep zone.

[1] All elevation datum throughout this report is North American Datum (NAD) 1927.

Torch Lake's recharge, precipitation, and groundwater inputs are the principal hydraulic inputs to the aquifer. Predominant hydraulic outputs are a lateral movement toward Lake Michigan with some leakage to the deep zone where sand is found in the confining bottom layer. However, due to insufficient monitoring and data suggesting this outflow is marginal, water losses to the deep zone are assumed to be negligible (GRT, 2019).

2.4 Climate

Antrim County is in the Northwest Lower climate region (Midwestern Regional Climate Center, 2012). This area experiences all four seasons but does not typically experience extreme weather events. The online climate database, NOWData (NOAA Online Weather Data), was used to collect historic climate data from 1926 to 2021 for monthly averages of temperature and precipitation. The closest weather station is located in East Jordan at the Bellaire, Antrim County Airport (KACB), located about 13 miles northeast of the project site. The average temperature for this period was approximately 45 °F (7.3 °C) showing a slight increase in temperature over the period (see Figure 2.3). The average precipitation for this period was approximately 4.35 inches (111 mm) (see Figure 2.4) (NWS & NOAA, 2021).

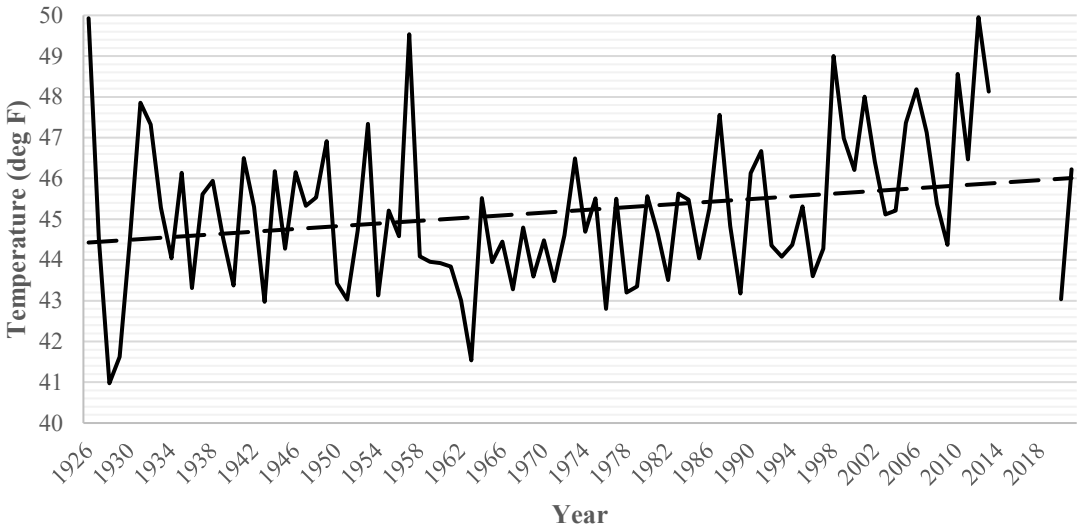

Figure 2.3: Average annual Temperature at Bellaire, Antrim County Airport (KACB) from 1926 to 2021. Data was accessed through the National Oceanic and Atmospheric Administration's National Weather Service NOWData.

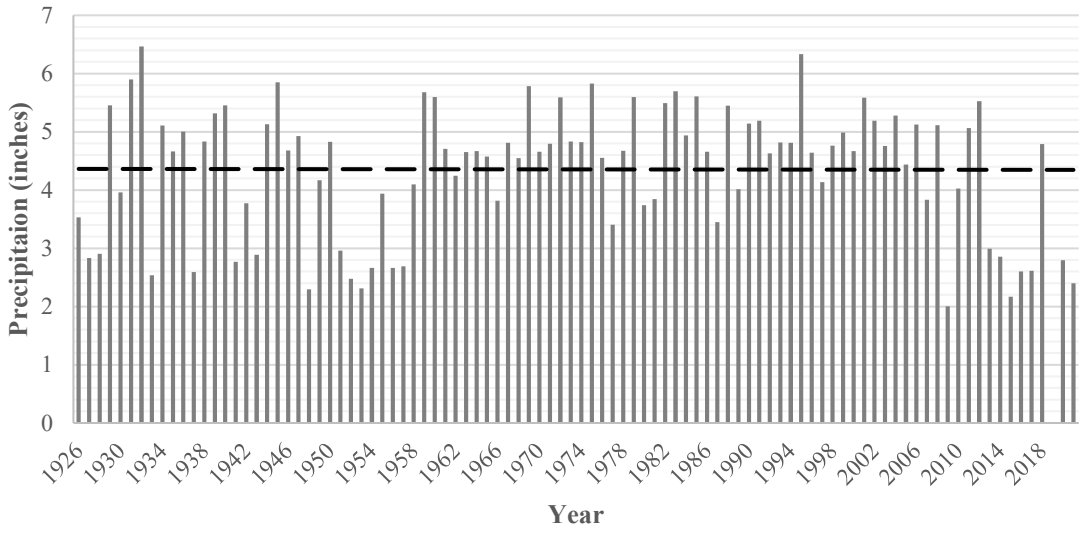

Figure 2.4: Average annual precipitation at Bellaire, Antrim County Airport (KACB) from 1926 to 2021. Data was accessed through the National Oceanic and Atmospheric Administration's National Weather Service NOWData.

2.5 Benzene, Toluene, Ethylbenzene, and Xylenes (BTEX)

Petroleum products are a frequent source of contamination to aquifers (Lu et al., 1999; Ritman et al., 2000, p. 69). Benzene, toluene, ethylbenzene, and isomers of xylene are often found co-currently within petroleum-derived plumes and, as stated previously, are often referred to as BTEX (Wilbur & Bosch, 2004). BTEX occurs naturally in crude oil, forest fires, and volcanic emissions and can be found in air, soil, and water. This contaminant can migrate and appear as soil gas in surrounding structures when present in groundwaters. Literature review has shown that each permutation of BTEX produces different toxic actions, so for this project, all four components will be considered for their joint toxic action (Lu et al., 1999; Taylor & Klotzbach, 2010; Wilbur et al., 2005; Wilbur & Bosch, 2004). The molecular structure of BTEX constituents are shown in Figure 2.5, and their physicochemical properties are listed in Table 2.1 (Mitra & Roy, 2011).

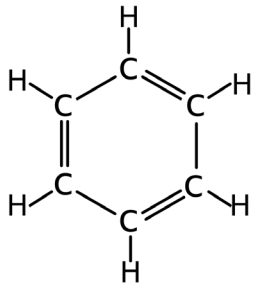

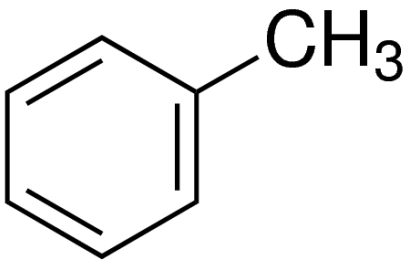

Benzene	Toluene

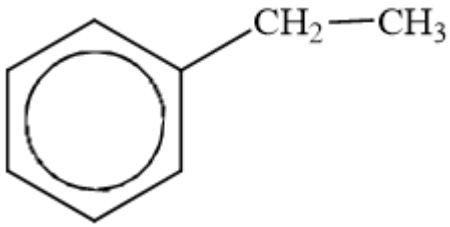

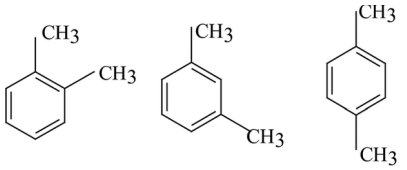

Ethylbenzene	Xylenes (left to right: o-xylene, m-xylene, p-xylene)

Figure 2.5: Molecular structure of benzene, toluene, ethylbenzene, and xylenes (o-xylene, m-xylene, and p-xylene) that comprise BTEX.

Table 2.1: Physicochemical properties/characteristics of BTEX (Mitra & Roy, 2011; New Jersey Department of Health, 2016; Taylor & Klotzbach, 2010; Wilbur et al., 2005).

Parameter	Benzene	Toluene	Ethylbenzene	Xylenes
Formula	C_2H_4	$C_6H_5CH_3$	$C_6H_5CH_2\ CH_3$	$C_6H_4(CH_3)_2$
Molar weight	78.12	92.15	106.18	106.18
Density (g/mL)	0.8765	0.8669	0.8670	0.8685
Polarity	Non-polar	Non-polar	Non-polar	Non-polar
Solubility (mg/L)	1780	500	150	150
Soil water partitioning coefficient, K_{oc}	97	242	622	570
Henry's Law Constant (25 °C) ($kPa \cdot m^3/mol$)	0.55	0.67	0.70	0.80
Odor	sweet-petrol like	solvent-like	petrol-like	faint, sweet
Color	clear, colorless	clear, colorless	clear, colorless	clear, colorless

2.5.1 Toxicology

Exposure pathways to BTEX are through inhalation of soil gas, ingestion of contaminated water, or direct dermal contact through an oil spill. Acute exposure can cause sensory and skin irritation, central nervous system problems (dizziness, headache, or coordination loss), and affect the respiratory system. Chronic exposure to high concentrations of BTEX can adversely affect internal organs, such as the kidney, liver, and blood systems (Mitra & Roy, 2011). Benzene is also classified by the National Toxicology Program as a human carcinogen and ethylbenzene is listed as a probable carcinogen (Wilbur et al., 2005; Wilbur & Bosch, 2004).

2.5.2 Environmental Fate

The transport and fate of BTEX are directly related to its chemical and physical properties as well as the attenuation media (air, water, and/or soil). In groundwater, the primary environmental fate is microbial degradation using both oxygen and nitrate as terminal electron acceptors (Li, 2017). Volatilization to the atmosphere can occur due to high vapor pressure and Henry's Law Constant. Photodegradation of the vapors can occur under sunlight (Li, 2017). Constituents of BTEX degrade rapidly in oxygen-rich settings, while degradation rates vary in anoxic (nitrogen-rich) environments (Schreiber & Bahr,

2002). Groundwater half-lives for BTEX under anaerobic conditions are on the order of years, with a hierarchy of benzene degrading faster than toluene, ethylbenzene, or xylenes (Bruce et al., 2010).

2.5.3 Regulatory Status

Regulatory standards for BTEX have been set separately by federal and state regulators to protect the environment and the public from the known adverse health effects these contaminants can have. The National Primary Drinking Water Regulations (NPDWR) are set by the US EPA and shown in Table 2.2.

Table 2.2: National Primary Drinking Water Regulations for BTEX constituents (US EPA, 2015).

Contaminant	Maximum Contaminant Level Goal (mg/L)	Maximum Contaminant Level (mg/L)
Benzene	0.0	0.005
Toluene	1.0	1.0
Ethylbenzene	0.7	0.7
Xylenes (total)	10	10

The release of hydrocarbons is regulated under Part 213 of the Natural Resources and Environmental Protection Act, P.A. 451 of 1994, as amended (Part 213). EGLE's (formerly Michigan Department of Environmental Quality (MDEQ) at the time the project began) leaking underground storage tank facility identification number associated with the project site is 0-0009190, and the facility ID for the underground storage tank is 50001467 (EGLE, 2013, 2020a; GRT, 2019). As of the most current documentation on analytes present at the site report levels of BTEX that are still exceeding the drinking water criteria (GRT, 2019, pp. 127–131).

The BTEX plume in Antrim County has heightened levels of contaminant still present in an aquifer that serves numerous residences and is attached to two important lakes, Lake Michigan and Torch Lake. The bioremediation of BTEX can be modeled initially to inform remediation design. This report seeks to model the effect of three bioremediation techniques on the known levels of BTEX in Antrim County.

3 Objectives

Modeling can often times be a cost-effective and time-efficient tool in planning site investigation when it comes to predicting groundwater flow and contaminant movement (Zengguang et al., 2015). Calibrated models can aid in the creation of pilot studies, monitoring plans, and remediation design of dangerous contaminants, like the BTEX plume in Antrim County. The overall goal of this project is to use modeling to help predict the effectiveness of three remediation techniques, natural attenuation, air injection, and EMB. The following objectives were developed to help guide this study towards that goal.

Objective 1: Construct and calibrate a regional flow model to simulate known hydraulic conditions.

Objective 2: Use the calibrated regional flow model to forecast aquifer behavior to simulate BTEX contamination extents and degradation due to natural attenuation, air injection, and EMB.

To achieve these objectives, literature-based methods and parameters as well as site-specific characterization are used to develop two models, a regional flow model and a transport model. The transport model will ultimately be used to simulate the three bioremediation techniques described above.

4 Methods

The industry-standard numerical modeling interface Groundwater Modeling System (GMS) Version 10.4.10 was utilized in this investigation. GMS is owned, managed, and distributed by AQUAVEO, LLC. AQUAVEO created this software platform in partnership with the Geographic Information System Company (ESRI), United States Army Corp of Engineers (USACE), and the Department of Transportation (DOT) in 2007 (Aquaveo, 2021a). This project utilized GMS for its ability to interface as a pre- and post-processor with an array of numerical modeling software, including MODFLOW, MODPATH, PEST, and MT3DMS.

MODFLOW was chosen as the three-dimensional groundwater modeling code utilized in this investigation. MODFLOW-2005 was re-released by the United States Geological Survey (USGS) in 2017 as an upgraded version of the modular model that had been evolving since 1988 (McDonald et al., 2003). A conceptual model depicting project parameters was developed using GIS datasets. Once the conceptual model is compiled in GMS, it is mapped to a grid for MODFLOW to compute a groundwater flow solution. The grid-based code simulates groundwater flow through the project extents by approximating the solution of the groundwater flow equation across the entirety of the grid cells for a variety of boundary conditions and hydrological processes such as recharge and pumping

The particle tracking code, MODPATH, is a USGS designed post-processor to MODFLOW (Pollock, 2016). MODPATH creates 3-D flow lines from the MOFLOW solution, demonstrating flow paths through the system. These flow paths serve as a visual representation of contaminant transport, denoting direction and velocity of travel.

Zheng developed a modular three-dimensional transport model multi-species (MT3DMS) in 1990 as a code that maps advection, dispersion, and basic chemical reactions to describe the fate and transport of constituents in groundwater (Zheng & Wang, 1998). This code mapped the initial concentrations of BTEX onto the 3-D grid created in GMS. Then it simulated the effect that natural attenuation, air injection, and EMB would have on the plume. The decay constants for the three biotechniques were varied in the basic chemical reaction package to match literature-based values.

Hydraulic conductivity and recharge values were calibrated using an automated parameter estimation (PEST) code in GMS. PEST optimizes parameters by varying its value iteratively until the simulated results resemble the observation data from wells in the system (Doherty, 2004). These calibrations help build confidence in the model by reducing mean error.

4.1 Conceptual Model

The GMS conceptual model approach was utilized as the framework for this investigation. The simplified conceptual model approach utilizes GIS tools to map sources, sinks, hydraulic boundaries, and other layer parameters to a conceptual model of the site (Aquaveo, 2021b). The conceptual model used one layer to model the unconfined

aquifer. The bottom elevation of the layer was assumed to be a constant 400 feet, approximately the depth of the diamicton that confines the lower aquifer. A 1-arcsecond DEM from the Advanced Spaceborne Thermal Emission and Reflection Radiometer (ASTER) was interpolated across the project surface to provide topology (NASA, 2004). The topography ranged in elevation between 575 and 665 feet. Recharge estimations were estimated from spatially distributed values from the Michigan Department of Natural Resources (DNR) and were constant across the project boundaries (DNR, 2019). The hydraulic conductivities were derived from the Quaternary map of this region (Farrand & Bell, 1998). Wellogic Water Wells were used to define groundwater-surface levels in observational wells and subsurface geology, finding the unconfined aquifer to be primarily comprised of sands and gravels. The confining unit at the bottom of the unconfined aquifer is primarily clays.

4.2 Boundary Conditions

In Torch Lake Township, the conceptual model covers approximately 0.5 square miles. The western boundary is bordered by the Lake Michigan shoreline and was defined as a constant hydraulic boundary with a head-stage of 574 feet (Keyhole, Inc., 2001). A constant hydraulic boundary with a head-stage of 591 feet of Torch Lake's shoreline comprised the eastern border (Keyhole, Inc., 2001). Both lakes vary seasonally and the chosen values represent average annual water levels. These boundaries were assigned as a specific head boundary condition with constant head values matching the physical hydraulic feature's water surface elevation. Boundary conditions are summarized in Table 4.1.

Table 4.1: Summary of boundary condition parameters in the conceptual model

Hydraulic Feature	Boundary Type Condition	Head *(feet)*
Lake Michigan	Specific Head	574
Torch Lake	Specific Head	591

A no-flow boundary was associated with the northern and southern borders to run parallel to the general groundwater flow from Torch Lake to Lake Michigan. Model calculations (and MODPATH flow lines) confirmed that these assumed boundaries did not affect the regional groundwater flow pattern due to their distance from the plume model and the similarity with the likely natural flow system. All cells outside of the model were inactivated.

4.2.1 Hydraulic Conductivity

The upper soils of the project site are composed of two main land systems, dune sand and coarse lacustrine deposits, composed of sand and gravel. Dune sand deposits are assumed to be homogeneous and isotropic. Lacustrine sand and gravel deposits are assumed to be homogeneous and isotropic with a lower hydraulic conductivity than that of dune sand. Constant rate pumping tests were performed on the coarse lacustrine material using

AQTESOLV Pro 4.5. While the physical soil is more complex than AQTESOLV can describe, AQTESOLV can provide a reasonable approximation of hydraulic conductivity for the project site. These approximations were utilized in choosing parameter values for the conceptual model prior to model calibration. An AQTESOLV solution for a slug test conducted on a monitoring well located within the plume extents, MW-20-01, is shown is Figure 4.1 with derived parameters in the following table (Table 4.2). The solution for this slug test is the Cooper-Bredehoeft-Papadopulos solution.

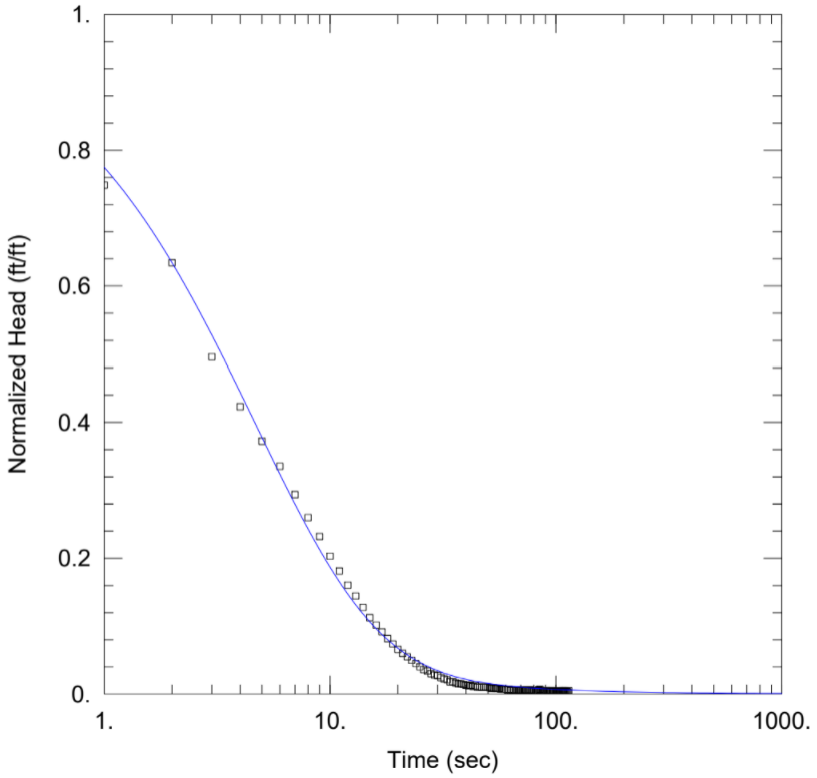

Figure 4.1: The solution for a slug test performed in well MW-20-01 using the Cooper-Bredehoeft-Papadopulos solution.

Table 4.2: Parameters derived from the Cooper-Bredhoeft-Papadopulos solution for a slug test performed in MW-20-01.

Parameter	Value
Transmissivity	10.86 cm^2/second
Storativity	0.0005417 (dimensionless)
Hydraulic Conductivity	67 ft/day

4.3 Recharge

The primary source of recharge to the project area is from precipitation and groundwater seepage from the Spencer Creek-Torch Lake watershed. Michigan's DNR found recharge

estimations across the project site at 10 in/year (0.0022 ft/day) (DNR, 2019). This recharge rate was utilized in the conceptual model prior to model calibration.

4.4 Regional Flow Model

This project utilized a steady-state flow model (Charbeneau, 2000, p. 94). The regional flow model used to model initial steady-state conditions consisted of 73 rows and 119 columns, with 5,279 active cells. The cells were uniformly 30 feet along the x- and y-extents. Layer geometry (varying topography from the DEM and a flat bottom at 400-ft elevation) dictated the thickness of each cell.

The flow model used steady-state calculations to determine the groundwater table. Due to sporadic groundwater level monitoring, average values for each observation well were chosen. The steady-state model then assumed that each of those wells was constant. By assuming that these static water levels remained constant over time, the model's run time and errors that could occur from inconsistent monitoring were both reduced.

Hydraulic conductivities were not considered isotropic as the upper soils changed from coarse lacustrine deposits to dune sand approximately halfway through the model (east to west). These two soil units were independently treated as isotropic and homogeneous. The starting heads for the initial simulation were set to equal the ground surface. The initial hydraulic conductivities were assumed from the land systems and were compared with approximations derived from slug tests performed on the project site, as described previously. The initial simulation used literature-based estimates of the hydraulic conductivity that were considered average values for the material type and DNR recharge estimates.

Darcy's Law of groundwater flow through porous earth media governs the solutions that MODFLOW calculates. MODFLOW uses the partial differential equation (Equation 1) to calculate 3-D groundwater flow (McDonald & Harbaugh, 1988).

Equation 1

$$\frac{\partial}{\partial x}\left(K_{xx}\frac{\partial h}{\partial x}\right)+\frac{\partial}{\partial y}\left(K_{yy}\frac{\partial h}{\partial y}\right)+\frac{\partial}{\partial z}\left(K_{zz}\frac{\partial h}{\partial z}\right)+W=S_s\frac{\partial h}{\partial t}$$

where,

K_{xx}, K_{yy}, and K_{zz} are values of hydraulic conductivity along the x, y, and z coordinate axes, which are assumed to be parallel to the major axes of hydraulic conductivity;
h is the potentiometric head;
W is a volumetric flux per unit volume and represents sources and/or sinks of water;
S_s is the specific storage of the porous material, and;
t is time.

The MODFLOW model setup is shown in Figure 4.2.

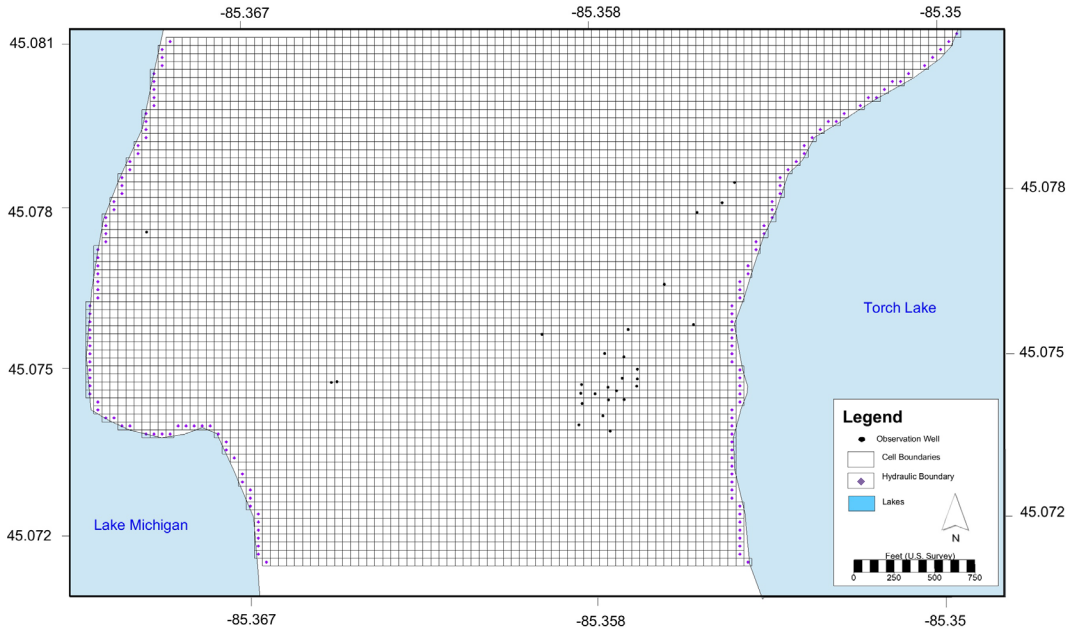

Figure 4.2: The MODFLOW model setup showing hydraulic boundaries, observation wells, and model boundaries.

4.5 Model Calibration

GMS PEST estimation was used to calibrate the MODFLOW model. Mean residual head, mean absolute head, and root mean squared error are all typically considered when calibrating a model. The PEST estimator runs iteratively, minimizing the statistical error between the observed and simulated heads. Following runs use the calibrated starting heads, rather than surface topography, as initial starting heads. MODFLOW calculates the mean error (ME) as a sum of the residual head and reflects the average error for the observation and is defined in Equation 2 (Aghlmand & Abbasi, 2019).

Equation 2

$$ME = \frac{1}{n}\sum_{i=1}^{n}(h_o - h_s)_i$$

where,
h_m is the observed head;
h_s is the simulated head;
n is the number of observation points, and;
ME is the mean error.

The mean absolute error (MAE) is a measure of the absolute value of the errors as defined below:

Equation 3

$$MAE = \frac{1}{n}\sum_{i=1}^{n} |(h_o - h_s)_i|$$

where,
h_m is the observed head;
h_s is the simulated head;
n is the number of observation points, and;
MAE is the mean absolute error.

The Root Mean Square (RMS) error, or standard deviation, describes the variation from the mean error and is calculated by averaging the squared differences in the computed and observed values.

Equation 4

$$RMS = [\frac{1}{n}\sum_{i=1}^{n} (h_o - h_s)_i^2]^{0.5}$$

where,
h_m is the observed head;
h_s is the simulated head;
n is the number of observation points, and;
RMS is the root mean square error.

4.6 Transport Modeling

Transport modeling was done using MT3DMS, a public domain code developed by Chunmiao Zheng in 1990 for the USEPA. This transport model accounts for advective and dispersive transport, linear partitioning, and chemical reactions. MT3DMS solves the three-dimensional partial differential equation (Equation 5) for advective-dispersive transport with partitioning and reaction for multicomponent plumes (Zheng & Wang, 1998).

Equation 5

$$\frac{\partial(\theta C^k)}{\partial t} = \frac{\partial}{\partial x_i}\left(\theta D_{ij}\frac{\partial C^k}{\partial x_j}\right) - \frac{\partial}{\partial x_i}(\theta v_i C^k) + q_s C_s^k + \sum R_n$$

where,
C^k is the dissolved concentration of species *k*;
Θ is the porosity of the subsurface medium, dimensionless;
t is time;

x_i is the dimension along the respective Cartesian coordinate axis;
D_{ij} is the hydrodynamic dispersion coefficient tensor;
V_i is the seepage or linear pore water velocity;
q_s is the volumetric flow rate per unit volume of aquifer representing fluid sources (positive) and sinks (negative);
C_s^k is the concentration of the source or sink flux for species k , and;
ΣR_n is the chemical reaction term.

MODFLOW simulated groundwater flow, and the velocities derived from the flow solution are used in the transport model for advection and hydrodynamic dispersion. Advection, dispersion, and retardation are all factors that affect mass transport (Charbeneau, 2000).

4.6.1 Advection

Advective transport is the movement of a solute due to bulk fluid movement and is typically the dominant influence in the transport of contaminants (Charbeneau, 2000, p. 293). Darcy's Law states that the average linear velocity describes groundwater flow through porous media. The following equation mathematically describes the average linear velocity:

Equation 6

$$v_x = \frac{K}{n_e}\left(\frac{dh}{dl}\right)$$

where,
v_x is a vector of the average linear velocity;
K is the hydraulic conductivity;
ne is the effective porosity (dmn.), and;
dh/dl is the hydraulic gradient.

4.6.2 Dispersion

Dispersion in porous media is defined as the spreading of the solute over a greater area that is not predicted by the average linear velocity due to heterogeneities in the media (Zheng & Wang, 1998). Analysis of scaling behavior for longitudinal dispersivity was conducted in the laboratory, in the field, and through computer modeling by Shulze-Makuch (Schulze-Makuch, 2005). Longitudinal dispersivity can be defined as the following equation:

Equation 7

$$\alpha = C(L)^m$$

where,
α is the longitudinal dispersivity;
c is a parameter characteristic for a geologic medium;
L is the flow distance, and;

m is the scaling exponent.

4.6.3 Diffusion

Movement due to random molecular motion will occur if a concentration gradient exists (Kirkwood et al., 1960). This movement is diffusion. Molecular diffusion and mechanical dispersivity are interdependent in groundwater flow and treated as a single term in the contaminant transport equation (Charbeneau, 2000, p. 365). The coefficient of hydrodynamic dispersion, DL, describes the relationship between molecular diffusion and mechanical dispersivity in the following equation:

Equation 8

$$D_L = \alpha_L v_x + D^*$$

where,
D_L is the longitudinal coefficient of hydrodynamic dispersion;
a_L is the dynamic dispersivity;
v_x is the average linear groundwater velocity, and;
D* is the effective molecular diffusion coefficient.

The diffusion effect is generally negligible and was not considered for this investigation.

4.6.4 Retardation

Retardation is a physical property of a contaminant that accounts for the decrease in contaminant velocity compared to that of the groundwater. This decrease is due to the time that the contaminant spends sorbed to the soil matrix and immobile (Charbeneau, 2000, p. 290). In GMS this dimensionless retardation factor is calculated as follows:

Equation 9

$$R = 1 + \rho \frac{K_d}{n}$$

where,
ρ is the dry bulk density;
K_d is the distribution coefficient or first sorption constant, and;
n is the dimensionless porosity.

While GMS takes sorption into account, the retardation factor is not simulated within this project. Therefore, all simulations of plume migration are conservative.

4.6.5 Chemical Transformations

In the particle tracking code, MT3DMS, is the chemical reaction package and it was used to model BTEX degradation. The rate constants varied depending on the remediation technique that were derived from the literary review, as shown in Table 4.3. Each constant applies to BTEX degradation as a completely mixed contaminant.

Table 4.3: BTEX remediation rate constants of the effect of natural attenuation, air injection, and enhanced microbial bioremediation are derived from literature.

Remediation Technique	Rate Constant (1/day)	Source
Natural Attenuation	0.02	(Wiedemeier et al., 1996)
Air Injection	0.04	(Vaezihir et al., 2012)
EMB	0.445	(Suarez & Rifai, 1999)

The effects of these different techniques were modeled as a change in the rate constant rather than modeling the technique explicitly. For example, injection of air would result in some volatilization of BTEX (air sparging) and the contact between the air and plume would likely not be perfect, but the MT3DMS is not a multiphase-fluid model, as it only simulates dissolved constituents in groundwater, so the intricacies of injecting a nonwetting, immiscible fluid (air) and the rate limitations for the transfer of oxygen from air into water were not accounted for in this work. One should presume that the modeling presented herein is a best-case scenario (El-Naas et al., 2014; Schreiber & Bahr, 2002).

Due to a lack of information regarding the subsurface soils, a sorption coefficient of zero was used, leading to conservative plume estimates. As sorption is negated, the MT3DMS model assumes that kinetic sorption is related to the first-order kinetic rate. When first-order kinetic rates are sufficiently high, MT3DMS assumes kinetic sorption is approaching equilibrium sorption. However, when the first-order kinetic rate is low, the sorption process is slower than the transport process resulting in a no sorption assumption in the model (Zheng & Wang, 1998, p. 198). Equation 10 describes the first-order reversible kinetic reaction that is used to describe sorption.

Equation 10

$$\rho_b \frac{\partial \bar{C}}{\partial t} = \beta(C - \frac{\bar{C}}{K_d})$$

where,
β is the first-order mass transfer rate between the dissolved and sorbed phases;
ρ_b is the bulk density of the subsurface medium;
$\bar{C}$ is the sorbed concentration;
C is the dissolved concentration, and;
K_d is the distribution coefficient.

The first-order irreversible rate reaction term is inserted into Equation 5 to replace the reaction constant ($\sum R_n$). This term is shown in Equation 11.

Equation 11

$$\sum R_n = -(\lambda_1 nC + \lambda_2 \rho_b \bar{C})$$

where,
λ_1 is the rate constant of the dissolved phase;
λ_2 is the rate constant of the sorbed phase;
ρ_b is the bulk density of the subsurface medium;
$\bar{C}$ is the sorbed concentration;
C is the dissolved concentration, and;
n is the dimensionless porosity of the subsurface medium.

4.7 Source of Contamination

As stated previously, the assumed source of the hydrocarbon plume is the underground storage tank that belonged to the Torch Lake Standard gas station. Monitoring of BTEX concentrations occurred from 2016 to 2018. While each organic constituent of BTEX degrades at an independent rate, this study seeks to model the plume as a lumped blend of BTEX. Thus, all BTEX starting concentrations are the summation of the known constituent concentration with the units of mg/L.

The rate constants for air injection and EMB are calculated in their corresponding literature using the molar concentration of BTEX. Thus, when summing the lump concentration of BTEX each component was first divided by its molecular weight and then the summation of the molar weight was divided by BTEX's formula weight. At maximum, only an 18% decrease in concentrations was observed between the summation based on mass and the summation based on molar concentration.

5 Results

5.1 Regional Flow Model

The result for the regional flow model steady-state simulation is shown in Figure 5.1. The general groundwater flow is westerly with a change in velocity across the topographic divide of the two land systems dune sand and coarse lacustrine material. The water surface drops 17 vertical feet over approximately 4,000 linear feet (0.43%). No groundwater divide is shown from the modeling and is verified by analytical modeling (Gierke, personal communication, 2022).

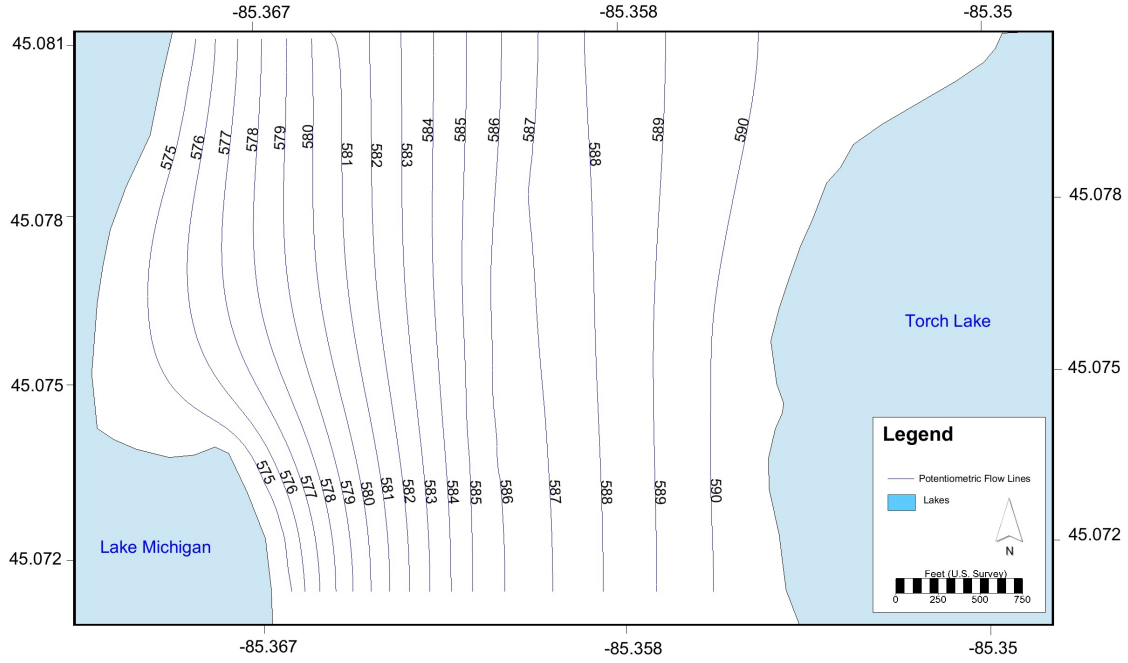

Figure 5.1: Potentiometric surface of the calibrated steady-state groundwater flow model.

5.2 Model Calibration

Few aquifer tests have been conducted in the shallow and intermediate aquifer to ascertain hydraulic conductivities. The driller's tests from well records can be used to approximate aquifer transmissivity and from those estimates, derive approximate values for hydraulic conductivity (Gierke, personal communication, 2022). That approach leads to variations in *HK* from less than 1 to just over 100 ft/day. Recharge estimates regionally and seasonally average about 10 inches/year. Lacking intentional measurements of recharge and hydraulic conductivities, model calibration was performed to better simulate the groundwater flow field by matching simulated and observed static water levels. The PEST simulation tool in GMS adjusted values of *HK* and recharge to minimize the difference between simulated and observed heads of the 26 monitoring wells found within the project site. These optimized values were then used to simulate a calibrated flow field, as shown in Figure 5.1. The initial and optimized hydraulic conductivities and

recharge values are shown in Table 5.1 and calibration statistics are shown in Table 5.2. The comparison of the observed and simulated heads is shown in Figure 5.2. The calibrated values were in the range of estimates from well records for *HK* (1-100 ft/day) and close to the reported regional/seasonal average of recharge.

Table 5.1: Optimized model parameters using automated parameter estimation (PEST) in MODFLOW.

Parameter	Initial Value *(ft/day)*	Optimized Value using PEST *(ft/day)*
HK_1 (dune sand)	51.0	30.0
HK_2 (coarse lacustrine deposits)	34.0	15.0
Recharge	0.0022	0.0017

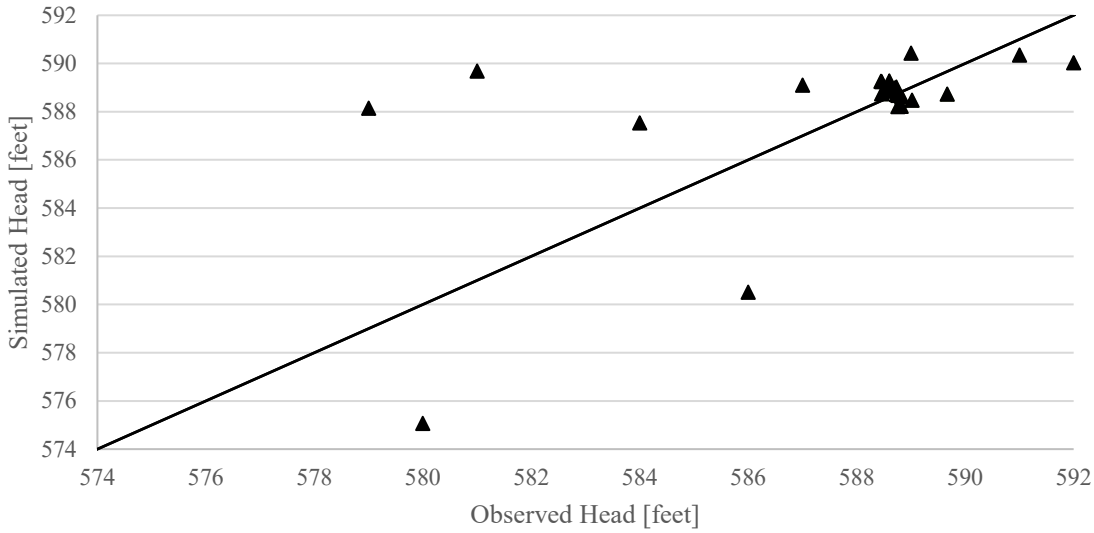

Figure 5.2: Comparison of calibrated MODFLOW-simulated head values of the static water level observations compared with known static water levels from project site well logs.

Table 5.2: Calibration statistics for PEST parameter estimation for the calibrated regional flow model.

Parameter	Value
Number of data points	26
Minimum Residual (Head)	0.0093[a]
Maximum Residual (Head)	9.15[b]
Mean Error (Residual Head)	-0.326
Mean Absolute Error (Residual Head)	1.888
Root Mean Squared Error (Residual Head)	3.133

[a] Well MW-17-06 which is located in the BTEX plume extents.
[b] Well ID 5000000313

5.3 Sensitivity Analysis

5.3.1 Hydraulic Conductivity and Recharge

A sensitivity analysis was performed on the initial hydraulic conductivities to test the impact calibration has on model results using PEST. PEST iteratively varies each parameter, hydraulic conductivity of dune sand and lacustrine material and recharge, to monitor their effect on the static water levels in the observation wells. Once the residual head, or the difference between the MODFLOW-simulated head and observed head, is minimized, PEST reports the new values for the input parameters. The calibrated model had a lower error than the initial model, showing that calibration successfully simulated static water level values closer to observed values. The initial simulated and observed values are compared in Figure 5.3, with statistics following in Table 5.3. Comparison can be made to calibrated statistics, shown in Table 5.2.

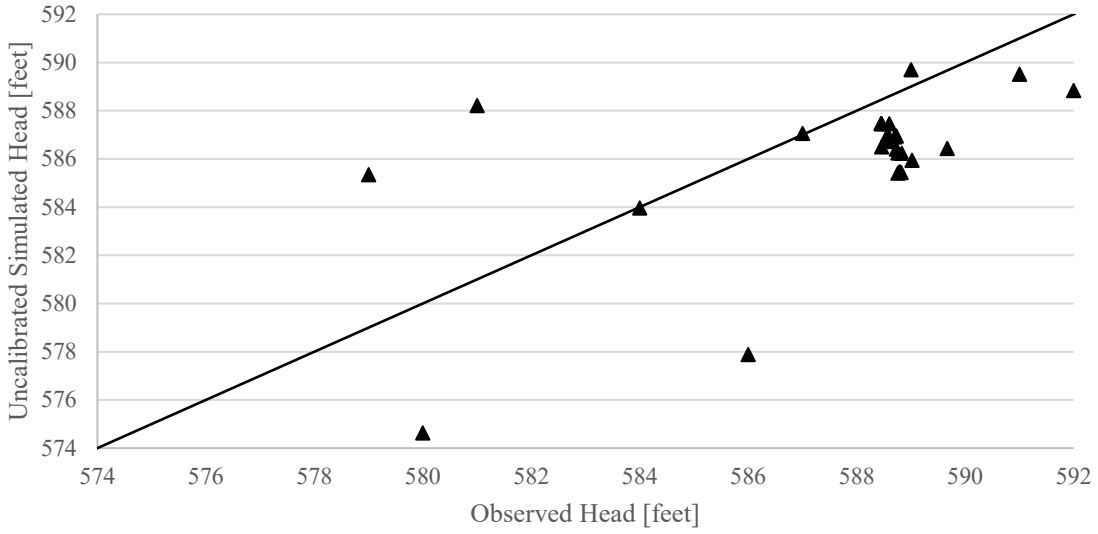

Figure 5.3: Comparison of uncalibrated MODFLOW-simulated head values of the static water level observations compared with known static water levels from project site well logs.

Table 5.3: Calibration Statistics for the uncalibrated regional flow model.

Parameter	Value
Number of data points	26
Minimum Residual (Head)	0.0337[a]
Maximum Residual (Head)	8.118[b]
Mean Error (Residual Head)	1.699
Mean Absolute Error (Residual Head)	2.801
Root Mean Squared Error (Residual Head)	3.462

[a] Well ID 5000001541
[b] Well ID 5000000310

The calibration of the model resulted in lower error, and better agreement between the simulated and observed values. To understand where the calibration had the largest effect, MODFLOW provides visual error bars to represent the residual head value. The distribution of the error over the 26 monitoring wells can be seen for the calibrated and uncalibrated models in Figures 5.4 and 5.5, respectively. A reduction of error is seen on the cluster of wells over the BTEX plume, near Torch Lake.

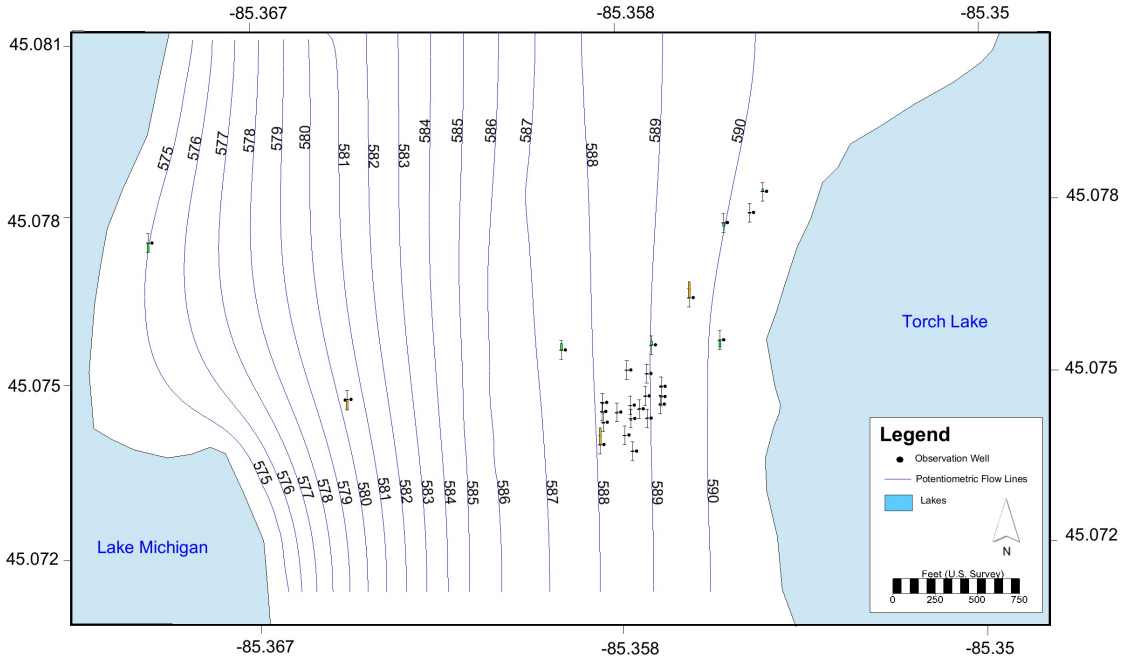

Figure 5.4: Distribution of error for the calibrated steady-state flow model. The error bars near the observation wells show the relative difference between the MODFLOW-simulated water levels and the observed water levels. Green, yellow, and red signify the residual of each well. Green is low error with the residual being less than five feet. Yellow is medium error with the residual below five and ten feet. Red is when the residual is above ten feet.

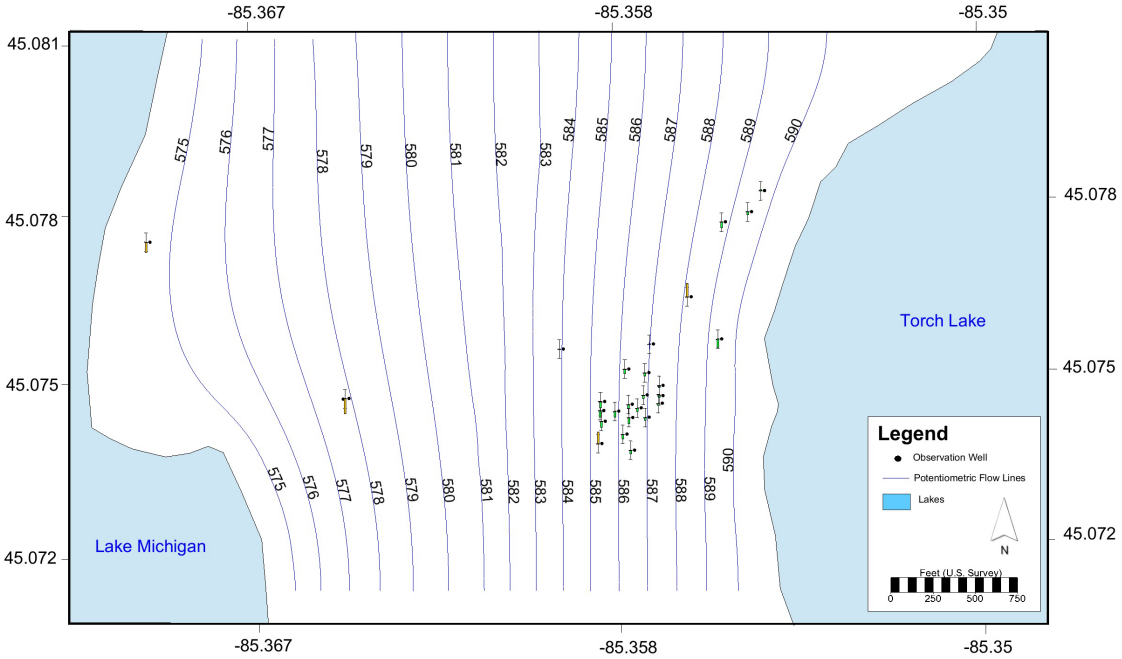

Figure 5.5: Distribution of error for the uncalibrated steady-state flow model. The error bars near the observation wells show the relative difference between the MODFLOW-simulated water levels and the observed water levels. Green, yellow, and red signify the residual of each well. Green is low error with the residual being less than five feet. Yellow is medium error with the residual below five and ten feet. Red is when the residual is above ten feet.

5.3.2 Decay Constants

Unlike the groundwater flow aspects of this work, where there are at least some site-specific observations to which to compare groundwater flow calculations to measured data, there were no site-specific data for biodegradation rates. To account for uncertainty of the decay constants, a sensitivity analysis was performed. The decay rates were compared to rates that were 20%, 50%, and 100% less than the used value ($K_{(nod)}$) as well as rates that were 20%, 50%, and 100% more than the used value ($K_{(nod)}$).

All of the transport models were sensitive to the change of the decay constant. Simulation of the varied decay rates were done using MT3DMS and were monitored at the epicenter of the plume (SB-17-02). The modified decay rates for natural attenuation, air injection, and EMB are shown in Figures 5.6, 5.7, and 5.8, respectively.

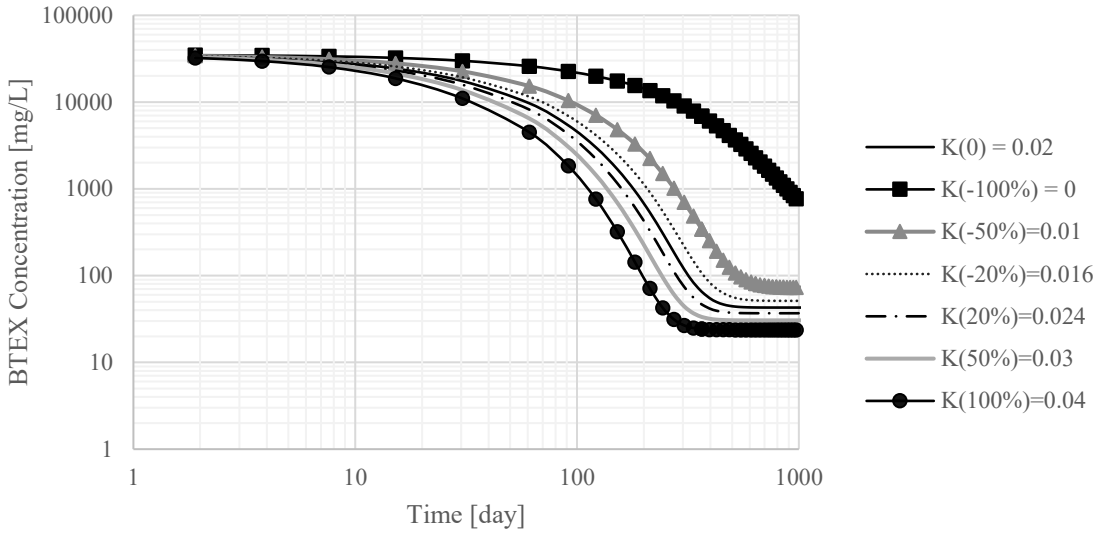

Figure 5.6: Sensitivity analysis for natural attenuation remediation. The decay constants for -20%, -50%, -100%, K(nod), 20%, 50%, and 100% are 0, 0.01, 0.016, 0.02, 0.024, 0.03, and 0.04 1/day, respectively.

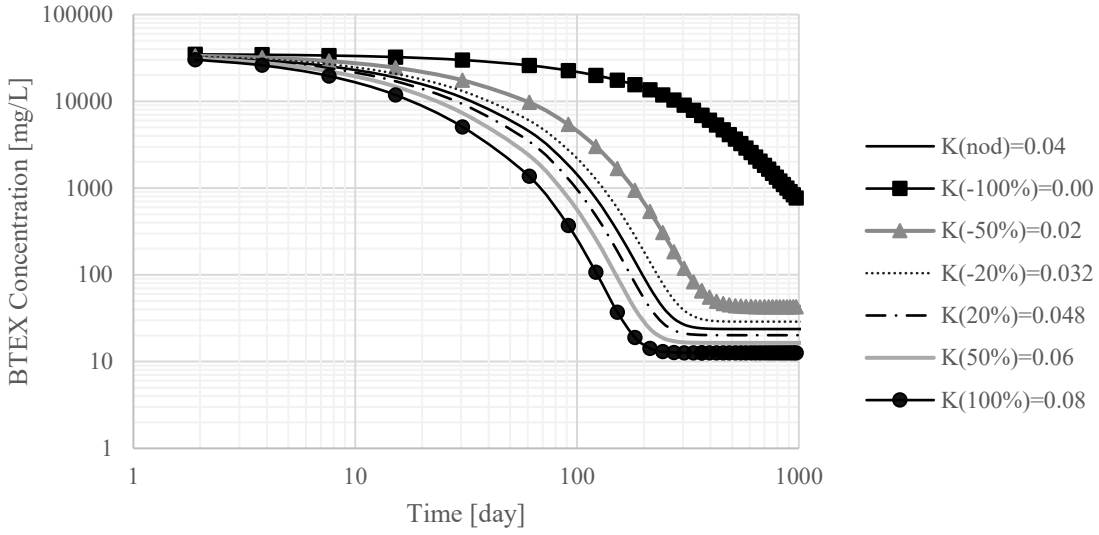

Figure 5.7: Sensitivity analysis for air injection remediation. The decay constants for -20%, -50%, -100%, K(nod), 20%, 50%, and 100% are 0, 0.02, 0.032, 0.04, 0.048, 0.06, and 0.08 1/day, respectively.

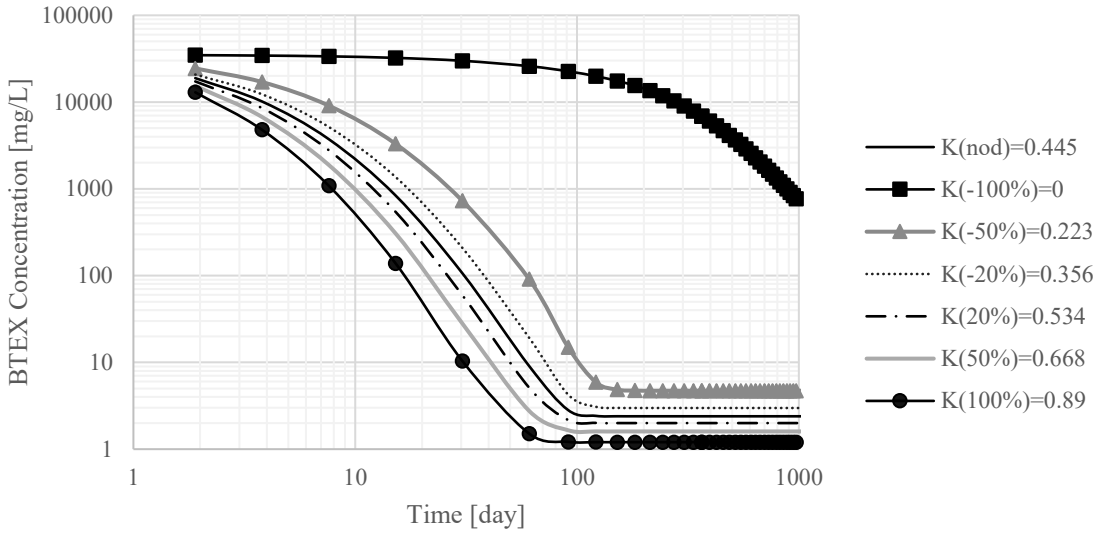

Figure 5.8: Sensitivity analysis for EMB. The decay constants for -20%, -50%, -100%, K(nod), 20%, 50%, and 100% are 0, 0.223, 0.356, 0.445, 0.534, 0.668, and 0.890 1/day, respectively.

5.4 Transport Modeling

Using the regional flow model solution from the calibrated MODFLOW simulations, MT3DMS was applied to the system to model the remediation of the BTEX plume using natural attenuation, air injection, and EMB. The parameters necessary for the MT3DMS modeling included starting BTEX concentrations, porosity, and decay constants. Five one-year periods simulated BTEX in the transient MT3DMS model. These stress periods were for output control and parameters were held constant throughout the different stress periods. Starting concentrations for BTEX were calculated using monitoring data taken from 2016 to 2018 (GRT, 2019, 2020). Given that no suitable measurements were taken across model extents, an average value of porosity for dune sand and lacustrine material, 0.3 (dimensionless), was used in transport modeling. The literature-based decay constant for natural attenuation, air injection, and EMB are 0.02 1/day, 0.04 1/day, and 0.445 1/day, respectively. MODPATH particle tracking was used as a visual indicator to show the direction of the contaminant transport. Further information on MODPATH particle tracking can be seen in Appendix 9.4.

When modeling the degradation of BTEX using first-order irreversible kinetic reactions, natural attenuation had the slowest degradation time followed by air injection. The fastest degradation time was that of EMB, which includes the addition of microbes as well as air. Figure 5.9 shows a comparison of the three remediation methods' efficiencies of plume degradation at the epicenter of the plume, at well SB-17-02. The chart is plotted with the ratio of concentration to initial concentration on the y-axis with time on the x-axis to compare the rate that each technique degraded BTEX. The rate of degradation for

all three converged as they reached an equilibrium and ceased to degrade the plume any further.

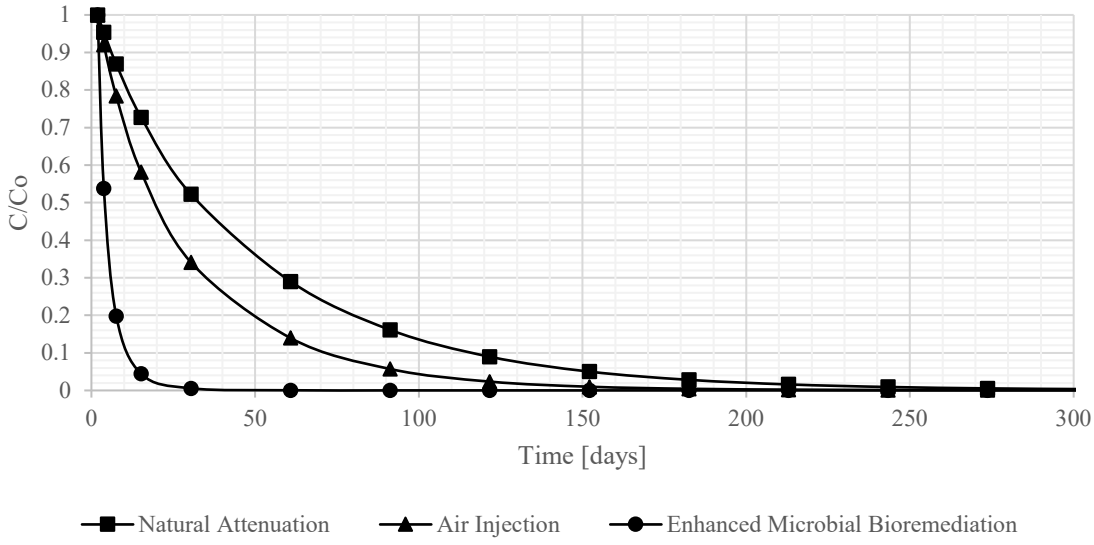

Figure 5.9: Comparison of natural attenuation, air injection, and enhanced microbial bioremediation efficiency of the degradation of a BTEX plume as recorded at SB-17-02.

Not only were the rates faster with additions of oxygen and microbes, but the extent of degradation was greater. Modeling these bioremediation techniques found that each treatment reached an equilibrium over time were they no longer degraded the plume. Natural attenuation remediation reached a steady state with a maximum residual BTEX concentration of 42.85 mg/L after 739 days. Air injection remediation reached a steady state with a maximum residual BTEX concentration of 23.72 mg/L after 578 days. Microbially enhanced bioremediation reached a steady state with a maximum residual BTEX concentration of 2.39 mg/L after 152 days. The rate at which the BTEX plume was degraded and reaches equilibrium can be seen in Figure 5.10. Please refer to Appendix 9.3 for additional images of the plume.

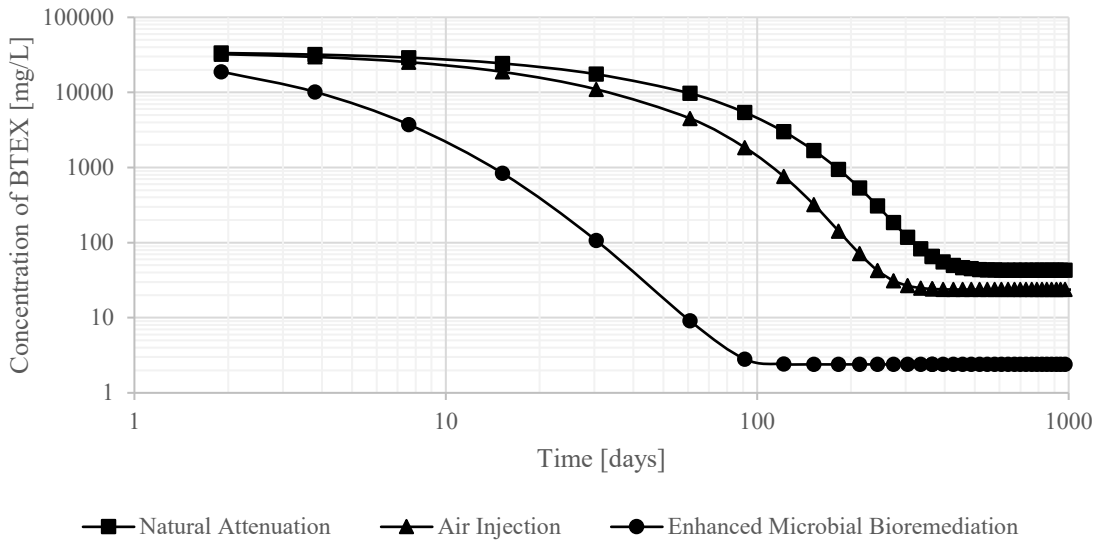

Figure 5.10: Comparison of degradation due to natural attenuation (squares), air injection (triangles), and EMB (circles). All three treatment techniques reached equilibrium.

While a conservative approach was taken for a few parameters associated with transport modeling (sorption and porosity), MT3DMS models the bioremediation as an ideal system. In reality, it would be unlikely to see consistent decay rates across the extent of the plume as heterogeneity in the subsurface may result in non-uniform mixing. Thus, the results of the transport model are considered an ideal solution and are not expected to be replicated in nature.

6 Discussion

6.1 Hydraulic Conductivity

The PEST optimized value for recharge was consistent with the reported estimated values from Michigan's DNR (0.0017 and 0.0022 ft/day). The PEST optimization varied from the assumed average values for the hydraulic conductivities of dune sand (30 and 51 ft/day) and coarse lacustrine deposits (15 and 34 ft/day). Hydraulic conductivity values are a function of the fluid and the media, thus span large ranges depending on grain sizes, grain-size distributions, packing/porosity, and surface textures (Freeze & Cherry, 1979, p. 28). For typical dune sand, particle size can range from 0.008 to 0.016 inches (Lopez & Missimer, 2020). For these particle ranges, hydraulic conductivity values range between 0.003 to 300 ft/day. For typical coarse lacustrine deposits, the particle size can range from 0.003 to 0.04 inches (Vaasma, 2008). For these particle ranges, hydraulic conductivity values range between 3 to 30,000 ft/day (Freeze & Cherry, 1979). PEST optimization results for these sediment materials fall within the associated hydraulic conductivity ranges and can be assumed as plausible values for the application of this model. However, further field testing is required to determine specific hydraulic conductivity values.

6.2 Remediation Design

The employment of EMB, as described herein, is supported by the results of model calculations as well as the following qualitative analysis. Out of the three remediation techniques modeled, this form of remediation projected the most reduced plume concentration. However, when choosing a remediation technique, cost, public preference, and remediation goals must also be assessed.

6.2.1 Cost

The cost associated with EMB accounts for capital, installation, operation, and maintenance costs. Capital costs would be any incurred costs that support the remediation effort. These costs may include the method used for microbial and amendment injection, groundwater monitoring wells, and other associated overhead costs. Total capital cost can range greatly depending upon the magnitude of the soil impact. Installation costs would include installing monitoring wells that also serve as injection and pumping wells. Operation and maintenance costs account for the money needed to run and maintain the system. These costs would account for the type of microbial slurry utilized. These slurries can vary depending on the time of year remediation will occur, the soil present, and the magnitude of the contamination (Kujat, 1999).

In total, the cost of biodegradation can be reasonably low. The only construction needed to complete the project are PVC wells, and all work is *in-situ,* which negates the expense of hauling sediment off-site.

6.2.2 Public Preference

The benefits of EMB include a relatively quick clean-up period, low construction needs, and minimal artifacts that remain on-site post-remediation. These factors bode well for surrounding residential areas as no excessive lengths of noise pollution should occur outside that of the pumps. Upon remediation completion, only low-profile wells should remain, causing minimal change to landscaping. For these reasons, enhanced microbial bioremediation is often seen as favorable by the public (Lach, 2003).

6.2.3 Remediation Goals

Treatment goals often concur with regulatory limits and recommendations set by the EPA. See section 2.5.3 to see the regulatory status of BTEX and its organic constituents.

6.3 Limitation and Uncertainty

The regional flow model produced a reasonable potentiometric surface. The input values for recharge and hydraulic conductivity were calculated based on assumptions of subsurface configuration (isotropic and homogeneous). While these values are consistent with reported averages, these values may vary significantly throughout the system and do not account for natural heterogeneity: further site parameterization and field sampling could allow for more complex modeling.

An intermediate confining layer was assumed to be located consistently at 400 feet. This assumption was based on publicly available borehole data and data provided by GRT. However, based on field reports, the confining layer is leaky in some locations and also varies throughout the project extents (GRT, 2020). Given the complexity associated with inter-aquifer drainage, a simplification of this layer was utilized in this project's scope.

Inside the investigation boundaries, one large capacity municipal well was identified. Bay Harbor is the owner of this well, and it serves approximately 51 seasonal residents. In estimating the average pumping of the well, it was assumed that each resident utilized 100 gallons of water a day. The community's need is 5,100 gallons of water per day for this population size. The well would need to pump continuously at 1.2 gallons per minute to provide enough water. The steady-state conceptual model did not include this well due to its seasonal nature and relatively low impact. Pumping from residential wells was also ignored due to the low impact these wells were assumed to have on the potentiometric surface.

6.4 Future Work

The conceptual model that was adopted for this work is a simplified hydrogeologic model based on publicly available data and data provided by GRT. Improvements could be made to the model by modeling the borehole data in GMS and using the associated horizons to determine the confining layer rather than modeling its extents at a continuous elevation. This improvement could modify the groundwater flow and increase confidence in the regional flow model. The heterogeneous representation of aquifer material in the

model could increase model sensitivity compared to that of the homogenous material assumed in this study. Heterogeneity, such as layering, would certainly impact the estimations of contaminant transport and degradations, potentially causing more spreading in the direction of flow.

The three different remediation methods are modeled to show the impacts of enhancement rather than model the particular injections of enhancements. Further modeling could be done to show how adding each component of the remediation technique could change the resulting plume degradation.

Additional BTEX monitoring could assist in plume transport and fate calibration. Known levels of contamination used for this study are from monitoring data between 2016 and 2018. Additional data could improve the kinetic constants utilized for natural attenuation.

7 Conclusions

The objectives of this study were to construct and calibrate groundwater flow and contaminant fate and transport models to aid in remediation design. The conceptual model approach utilized public and private data to create the regional flow model. Modeling using the calibrated parameters showed relatively consistent results with known static water levels across the site. The fate and transport of the BTEX plume were projected using the known contamination levels and the groundwater flow model. The model results are consistent with general understanding of reactive-plume behavior, but there are currently no measured data to calibrate the contaminant remediation for the site at this time (Vaezihir et al., 2012; Zengguang et al., 2015).

Using literature-based approaches and parameters, three bioremediation techniques (natural attenuation, air injection, and EMB) were simulated to test contaminant remediation. The modeling found that EMB decreased the BTEX plume the most, with the maximum residual BTEX concentration being 2 mg/L. Air injection and natural attenuation also decreased the plume so that the maximum residual BTEX concentrations were 24 mg/L and 43 mg/L, respectively.

This project has demonstrated the benefits of modeling site characteristics to plan pilot testing and help inform remediation design. Modeling is a low-cost technique that allows for a variety of remediation designs to be vetted before more cost-intensive methods are carried out. While modeling is not meant to be the sole consideration in choosing treatment techniques, it can be used concurrently with value engineering and site investigation to provide a holistic approach to remediation design. The incorporation of modeling in remediation design could potentially lead to time-efficient and cost-effective engineering practices.

8 Reference List

Aghlmand & Abbasi. (2019). Application of MODFLOW with Boundary Conditions Analyses Based on Limited Available Observations: A Case Study of Birjand Plain in East Iran. *Water*, *11*(9), 1904. https://doi.org/10.3390/w11091904

Antrim County Michigan. (2017). *Parcel Maps—Current Property Class* [Map].

Apple, B. A., & Reeves, H. W. (2007). *Summary of Hydrogologic Conditions by County for the State of Michigan* (Open-File Report, p. 78) [U.S. Geological Survey Open-File Report 2007-1236].

Aquaveo. (2021a). *About Us*. https://www.aquaveo.com/about-us

Aquaveo. (2021b). *GMS - Groundwater Modeling System*. https://www.aquaveo.com/software/gms-groundwater-modeling-system-introduction

ATSDR. (2021). *Recommendation for Exposure-Based Assessment of Joint Toxic Action of the Mixture*. Agency for Toxic Substances and Disease Registry. https://www.atsdr.cdc.gov/interactionprofiles/ip-btex/ip05-c3.pdf

Bedekar, V., Morway, E. D., Langevin, C. D., & Tonkin, M. (2016). *MT3D-USGS Version 1: A U.S. Geological Survey Release of MT3DMS Updated with New and Expanded Transport Capabilities for Use with MODFLOW* (Techniques and Methods) [Techniques and Methods].

Bruce, L., Kolhatkar, A., & Cuthbertson, J. F. (2010). *Comparison of BTEX Attenuation Rates Under Anaerobic Conditions*. *3*, 17.

Charbeneau, R. (2000). *Groundwater Hydraulics and Pollutant Transport*. Waveland Press, Inc.

DNR. (2019). *Estimated Groundwater Recharge*. https://gis-midnr.opendata.arcgis.com/datasets/midnr::estimated-groundwater-recharge/about

Doherty, J. (2004). *PEST: Model-Independet Parameter Estimation* (5th Edition; User Manual, p. 336). http://gmsdocs.aquaveo.com/pest.pdf

EGLE. (2013). *EGLE - Cleanup Criteria Requirements for Response Activity (Formerly the Part 201 Generic Cleanup Criteria and Screening Levels)*. https://www.michigan.gov/egle/0,9429,7-135-3311_4109-251790--,00.html

EGLE. (2020a). *GROUNDWATER: RESIDENTIAL AND NONRESIDENTIAL PART 201 GENERIC CLEANUP CRITERIA AND SCREENING LEVELS*.

EGLE. (2020b). *Watershed Boundary—12 Digit*. https://gisago.mcgi.state.mi.us/arcgis/rest/services/OpenData/hydro/MapServer/20

EGLE. (2022). *GeoWebFace Map Page* [Database]. http://www.deq.state.mi.us/geowebface/

El-Naas, M. H., Acio, J. A., & El Telib, A. E. (2014). Aerobic biodegradation of BTEX: Progresses and Prospects. *Journal of Environmental Chemical Engineering*, *2*(2), 1104–1122. https://doi.org/10.1016/j.jece.2014.04.009

Farrand, W. R., & Bell, D. L. (1998). *Quaternary Geology of Michigan* [Map]. https://mnfi.anr.msu.edu/data/quaternary-geology/antrim.pdf

Freeze, & Cherry. (1979). *Groundwater*. Pearson Publisher. http://hydrogeologistswithoutborders.org/wordpress/1979-english/

Gierke, J. S. (2022). *Personal communication with Dr. John Gierke regarding analytical modeling of BTEX plume in Torch Lake. Gierke has used the site as a homework project for the groundwater engineering course at MTU.* [Personal Communication].

GRT. (2019). *Remedial Investigation Report*.

GRT. (2020). *2020 ISCO Pilot Study Timeline*.

Haynes, J. K. (2011). *Ch. 14 Michigan Environmental Protection Act—Environmental Law Section*. https://connect.michbar.org/envlaw/reports/deskbook/chapter14

Keyhole, Inc. (2001). *Google Earth Pro* [Windows]. Google.

Kirkwood, J. G., Baldwin, R. L., Dunlop, P. J., Gosting, L. J., & Kegeles, G. (1960). Flow Equations and Frames of Reference for Isothermal Diffusion in Liquids. *The Journal of Chemical Physics*, *33*(5), 1505–1513. https://doi.org/10.1063/1.1731433

Kujat, J. D. (1999). A Comparison of Popular Remedial Technologies for Petroleum Contaminated Soils from Leaking Underground Storage Tanks. *Electronic Green Journal*, *1*(11). https://doi.org/10.5070/G311110353

Lach, D. (2003). *Eliciting Public Attitudes Regarding Bioremediation Cleanup Technologies: Lessons Learned from a Consensus Workshop in Idaho* (No. 837162; p. 837162). https://doi.org/10.2172/837162

Landmeyer, J. E., & Bradley, P. M. (2003). Effect of Hydrologic and Geochemical Conditions on Oxygen-Enhanced Bioremediation in a Gasoline-Contaminated Aquifer. *Bioremediation Journal*, *7*(3–4), 165–177. https://doi.org/10.1080/713607983

Li, X. D. and Y. (2017). Sources and Fates of BTEX in the General Environment and Its Distribution in Coastal Cities of China. *Journal of Environmental Science and Public Health*, *1*(2), 86–106.

Lopez, & Missimer. (2020). Statistical comparisons of grain size characteristics, hydraulic conductivity, and porosity of barchan desert dunes to coastal dunes. *Aeolian Research*, *43*(100576). https://doi.org/10.1016/j.aeolia.2020.100576

Lu, G., Clement, T. P., Zheng, C., & Wiedemeier, T. H. (1999). Natural Attenuation of BTEX Compounds Model Development and Field-Scale Application. *Groundwater*, *37*(5).

McDonald, M. G., & Harbaugh, A. W. (1988). A Modular Three-Dimensional Finite-Difference Ground-Water Flow Model. In *Techniques of Water-Resources Investigations of the United States Geological Survey*. https://pubs.usgs.gov/twri/twri6a1/pdf/twri_6-A1_a.pdf

McDonald, M. G., Harbaugh, A. W., & Modflow, T. O. A. O. (2003). The History of MODFLOW. *Groundwater*, *41*(2), 280–283. https://doi.org/10.1111/j.1745-6584.2003.tb02591.x

MDEQ. (2005). *Bedrock Geology of Michigan* [Map]. https://www.michigan.gov/documents/CGI_1987_Bedrock_Geology_8X11_128879_7.pdf

Midwestern Regional Climate Center. (2012). *Historical Climatology: Northwest Lower Michigan*.

https://glisa.umich.edu/media/files/climaticdivs/michigan/Michigan_Climatic_Division_3.pdf
Mitra, S., & Roy, P. (2011). BTEX: A Serious Ground-water Contaminant. *Research Journal of Environmental Sciences*, *5*(5), 394–398. https://doi.org/10.3923/rjes.2011.394.398
NASA. (2004). *ASTER Global Digital Elevation Map*. https://asterweb.jpl.nasa.gov/gdem.asp
NWS & NOAA. (2021, January 21). *NOWData—NOAA Online Weather Data for East Jordan*. National Weather Service; NOAA's National Weather Service. https://www.weather.gov/wrh/Climate?wfo=apx
Pollock, D. W. (2016). *User guide for MODPATH Version 7- A particle-tracking model for MODFLOW: U.S. Geological Survey Open-File Report 2016-1086* (Open-File Report, p. 35) [Open-File Report].
Ritman, Barden, & Bekins. (2000). Scientific Basis for Natural Attenuation. In *Natural Attenuation for Groundwater Remediation*. National Academics Press. https://www.nap.edu/read/9792/chapter/1#ii
Schreiber, M. E., & Bahr, J. M. (2002). Nitrate-enhanced bioremediation of BTEX-contaminated groundwater: Parameter estimation from natural-gradient tracer experiments. *Journal of Contaminant Hydrology*, *55*(1–2), 29–56. https://doi.org/10.1016/S0169-7722(01)00184-X
Schulze-Makuch, D. (2005). Longitudinal dispersivity data and implications for scaling behavior. *Groundwater*, *43*(3), 443–456. https://doi.org/10.1111/j.1745-6584.2005.0051.x
Suarez, M. P., & Rifai, H. S. (1999). Biodegradation Rates for Fuel Hydrocarbons and Chlorinated Solvents in Groundwater. *Bioremediation Journal*, *3*(4), 337–362. https://doi.org/10.1080/10889869991219433
Taylor, J., & Klotzbach, J. (2010). *Toxicological Profile for Ethylbenzene*. Agency for Toxic Substances and Disease Registry.
Vaasma, T. (2008). Grain-size analysis of lacustrine sediments: A comparison of pre-treatment methods. *Estonian Journal of Ecology*, *57*, 231–243. https://doi.org/10.3176/eco.2008.4.01
Vaezihir, A., Zare, M., Raeisi, E., Molson, J., & Barker, J. (2012). Field-Scale Modeling of Benzene, Toluene, Ethylbenzene, and Xylenes (BTEX) Released from Multiple Source Zones. *Bioremediation Journal*, *16*(3), 156–176. https://doi.org/10.1080/10889868.2012.687415
Wiedemeier, T. H., Swanson, M. A., Wilson, J. T., Kampbell, D. H., Miller, R. N., & Hansen, J. E. (1996). Approximation of Biodegradation Rate Constants for Monoaromatic Hydrocarbons (BTEX) in Ground Water. *Groundwater Monitoring & Remediation*, *16*(3), 186–194. https://doi.org/10.1111/j.1745-6592.1996.tb00149.x
Wilbur, S., & Bosch, S. (2004). *Interaction Profile for: Benzene, Toluene, Ethylbenzene, and Xylenes (BTEX)*. Agency for Toxic Substances and Disease Registry (ATSDR). https://www.atsdr.cdc.gov/interactionprofiles/ip-btex/ip05.pdf

Wilbur, S., Keith, S., Faroon, O., Wohlers, D., Stickney, J., Paikoff, S., Diamond, G., & Quinones, A. (2005). *Toxicological Profile For Benzene*. Agency for Toxic Substances and Disease Registry.

Zengguang, X., Li, Y., Junrui, C., Qin, R., & Rong, Y. (2015). Bioremediation Modeling of an Aquifer Contaminated by Benzene Using the Slow-Release Oxygen Source Technique. *Arabian Journal for Science and Engineering*, *40*. https://doi.org/10.1007/s13369-015-1637-6

Zheng, C., & Wang, P. (1998). *MT3DMS: A Modular Three-Dimensional Multispecies Transport Model* (SERDP-99; Documentation and User's Guide, p. 239). Defense Technical Information Center. https://doi.org/10.21236/ADA338509

9 Appendix

9.1 Well Data used for Model Calibration

Table 9.1: Well data from Wellogic well logs and monitoring data from GRT (GRT, 2019).

Well ID	Observed Head *(feet)*	Simulated Head *(feet)*	Uncalibrated Simulated Head *(feet)*
5000002091	580	575.07	574.63
5000000311	591	N/A	N/A
5000000310	586	580.54	577.88
5000004961	589	590.43	589.69
5000005146	591	590.35	589.52
5000002515	592	590.03	588.84
5000004395	581	589.69	588.21
5000004810	594	590.26	589.46
5000000313	579	588.15	585.35
5000001541	584	587.53	583.97
5000005318	587	589.09	587.06
MW-16-04	588.76	588.67	586.25
MW-18-07	588.73	589.02	586.96
MW-18-05	588.60	589.27	587.47
MW-19-02M	588.45	589.26	587.47
MW-17-09	588.70	588.99	586.92
MW-17-06	588.73	588.72	586.41
MW-17-08	588.57	588.88	586.72
MW-18-01	588.46	589.25	587.46
MW-17-07	588.57	589.02	587.01

MW-17-05	589.67	588.72	586.44
MW-17-03	588.83	588.61	586.24
MW-18-02	588.46	588.74	586.51
MW-5	588.79	588.22	585.47
MW-16-03	588.76	588.21	585.41
MW-17-01	589.02	588.48	585.94

9.2 Analyte Data for BTEX constituents at Project Site in Torch Lake, Antrim County

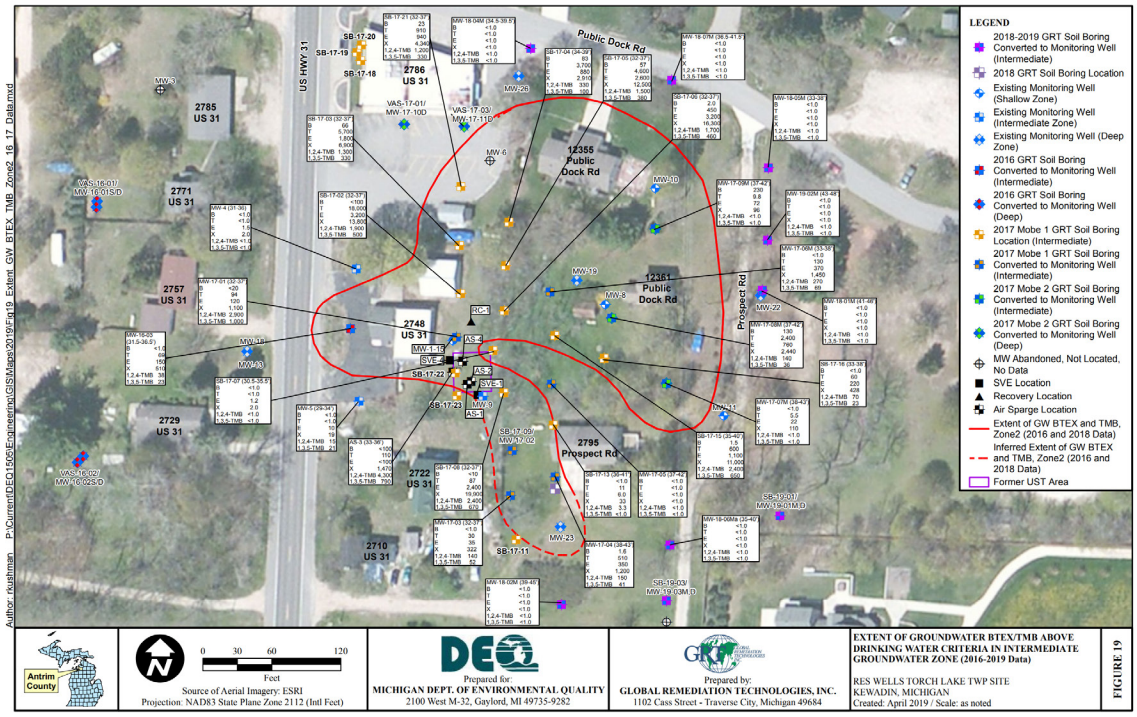

Figure 9.1: Analyte data for BTEX constituents within the project site boundaries (GRT, 2019).

9.3 Figures of MT3DMS simulated plume extents for natural attenuation, air injection, and enhanced microbial bioremediation.

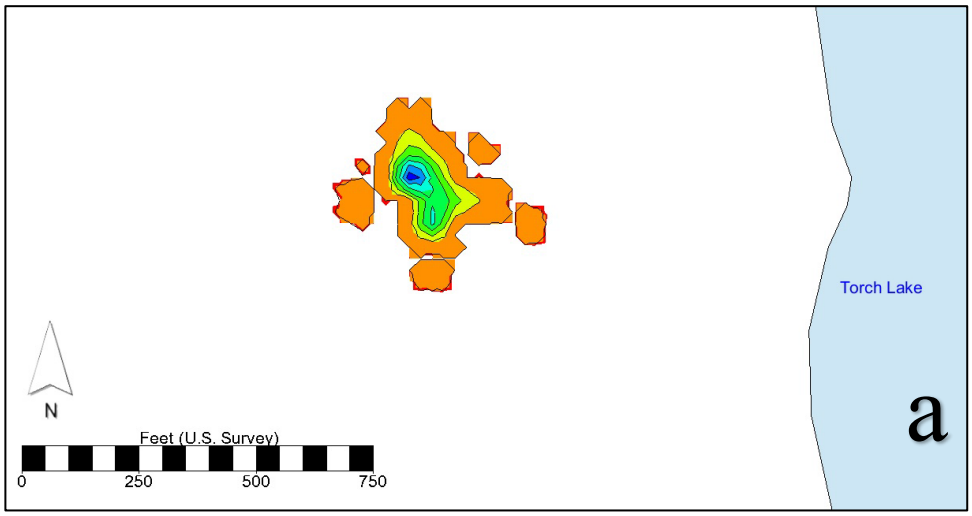

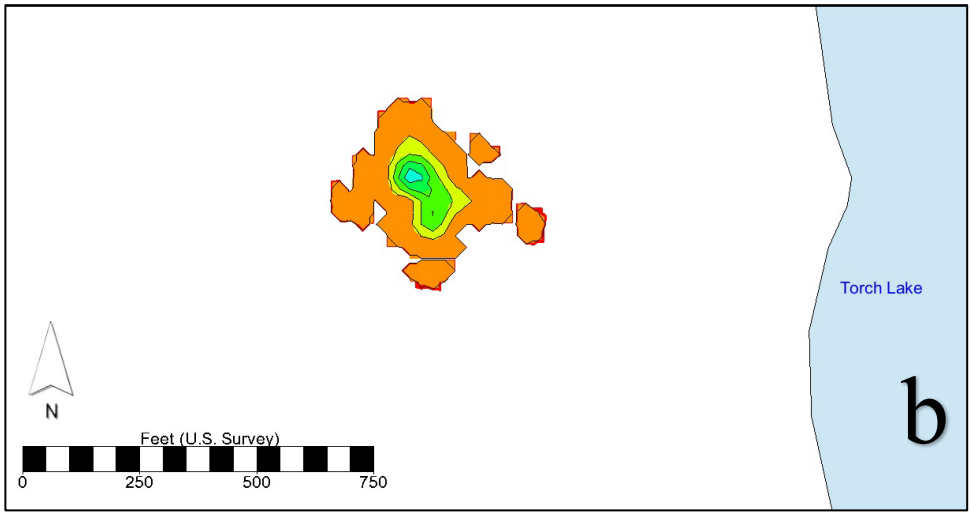

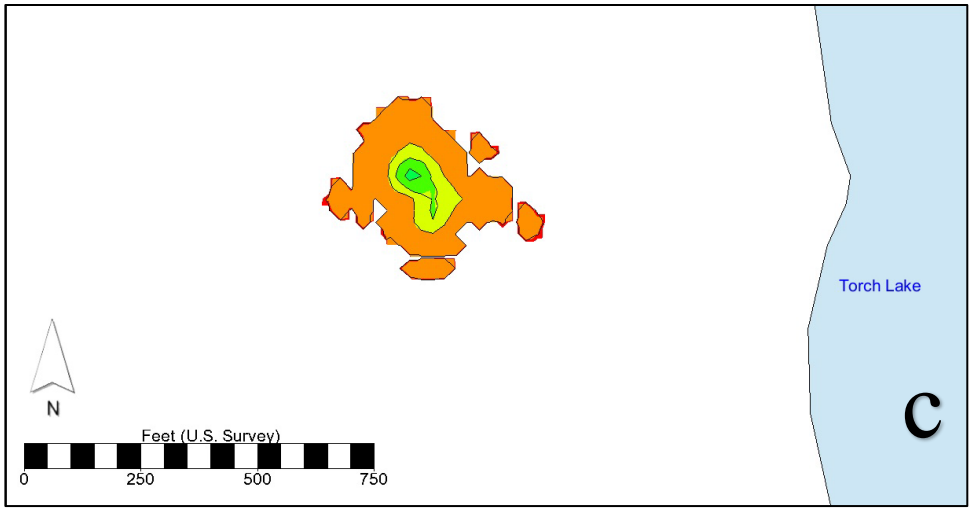
Torch Lake
c
N
Feet (U.S. Survey)
0
250
500
750

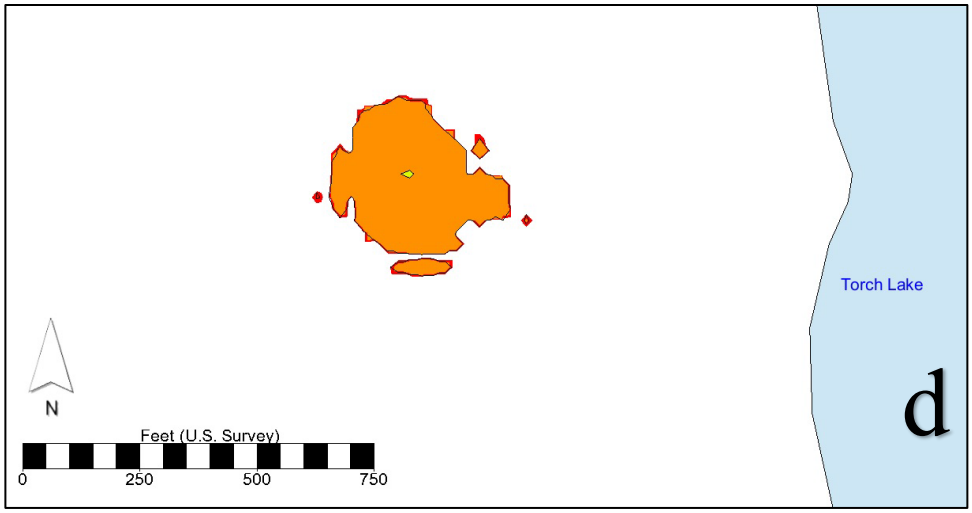
Torch Lake
d
N
Feet (U.S. Survey)
0
250
500
750

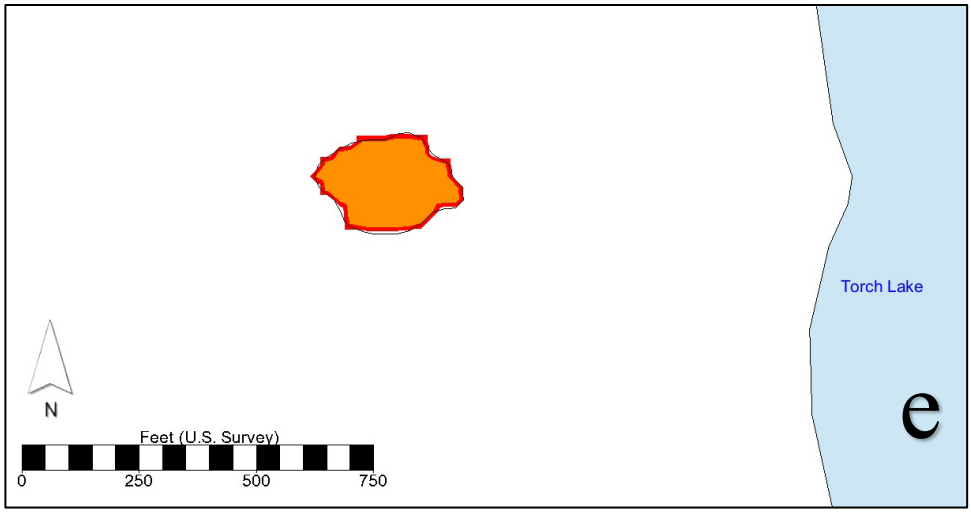
Torch Lake
e
N
Feet (U.S. Survey)
0
250
500
750

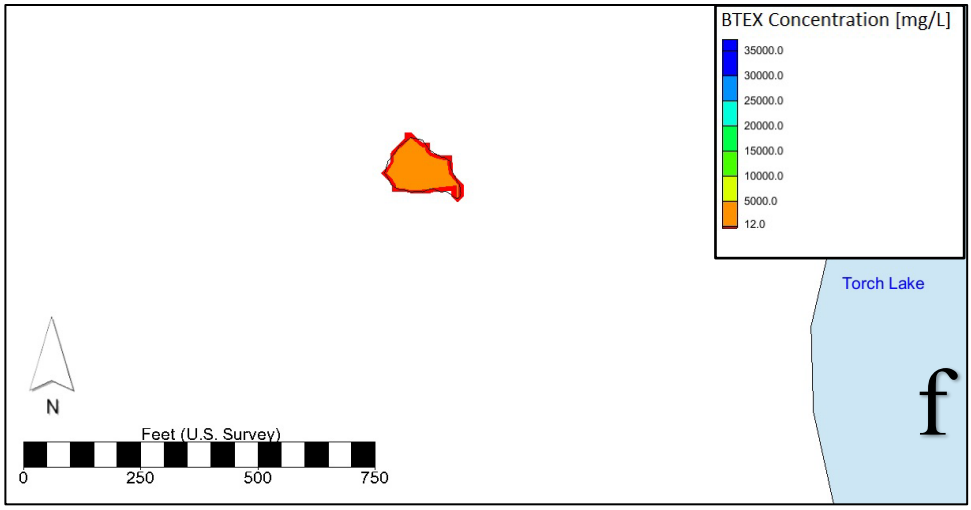

Figure 9.2: MT3DMS simulated plume extents for natural attenuation remediation at 1 (a), 15 (b), 30 (c), 60 (d), 90 (e), and 740 (f) days. The lowest shown contour is 12 mg/L.

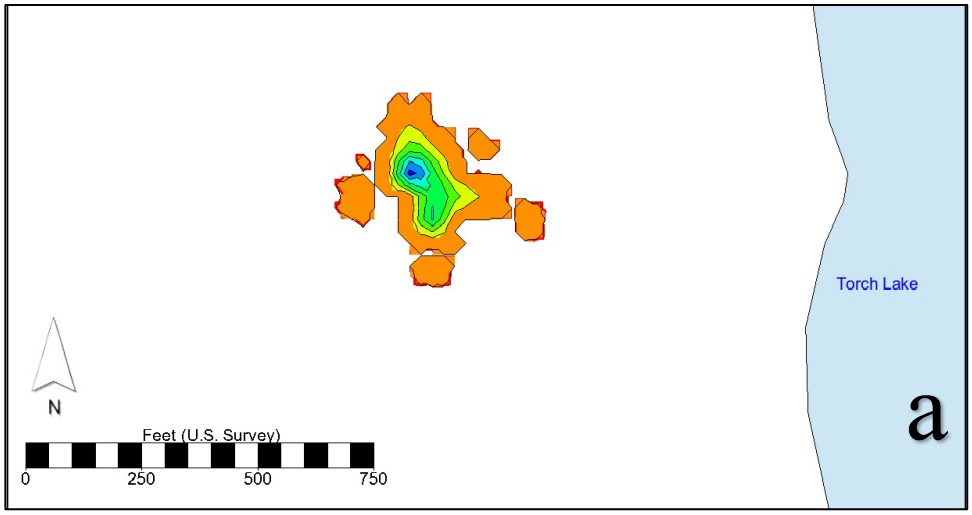
Torch Lake
N
Feet (U.S. Survey)
0
250
500
750
a

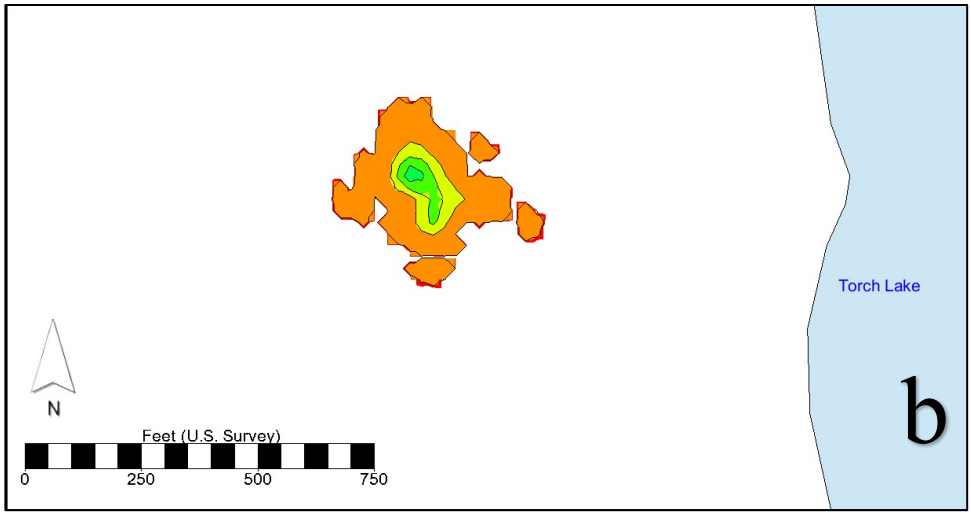
Torch Lake
N
Feet (U.S. Survey)
0
250
500
750
b

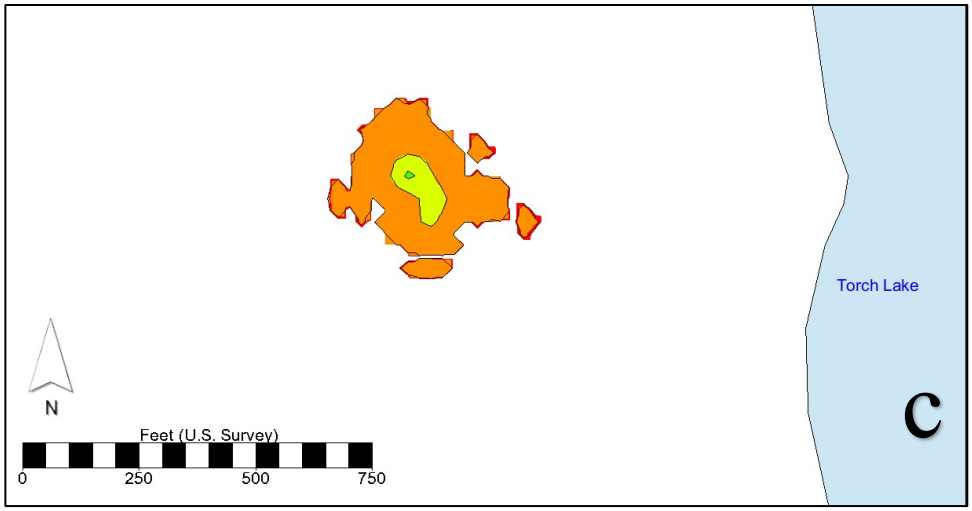
Torch Lake
c
N
Feet (U.S. Survey)
0
250
500
750

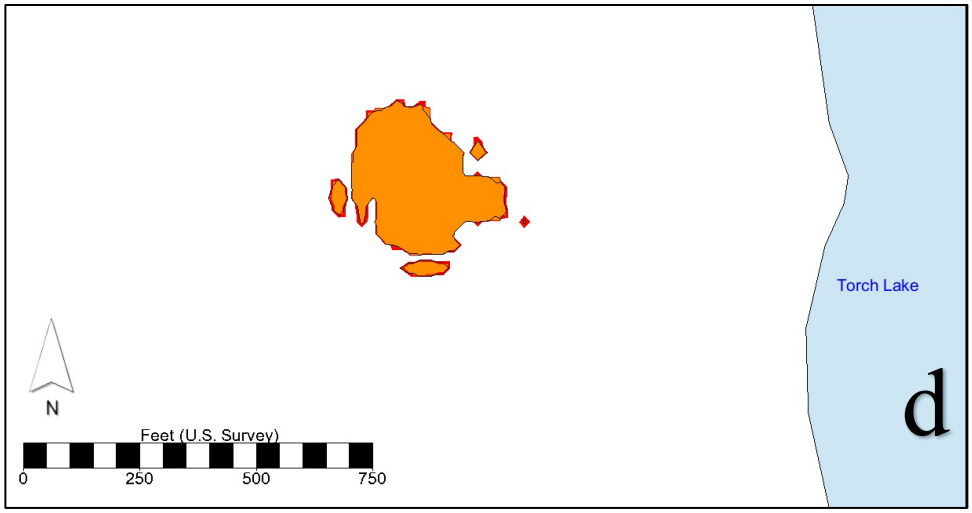
Torch Lake
d
N
Feet (U.S. Survey)
0
250
500
750

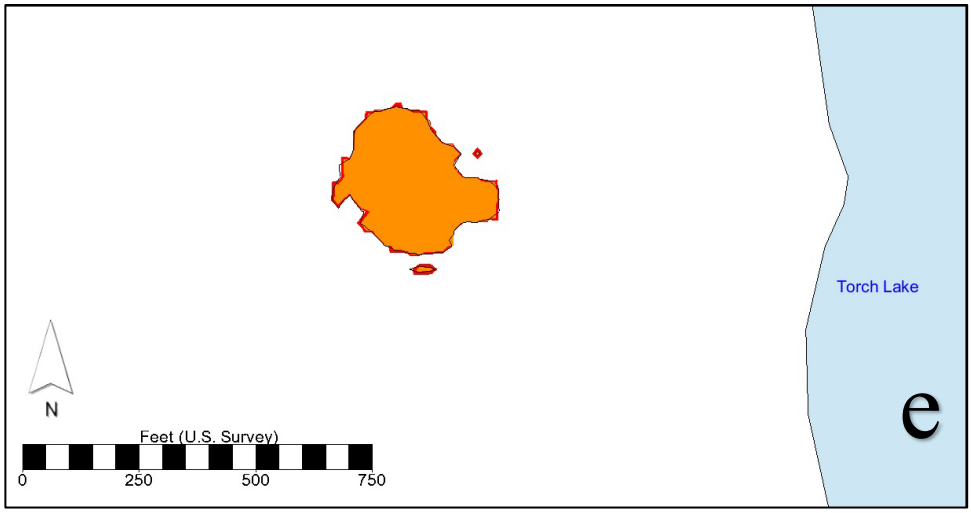
Torch Lake
e
N
Feet (U.S. Survey)
0
250
500
750

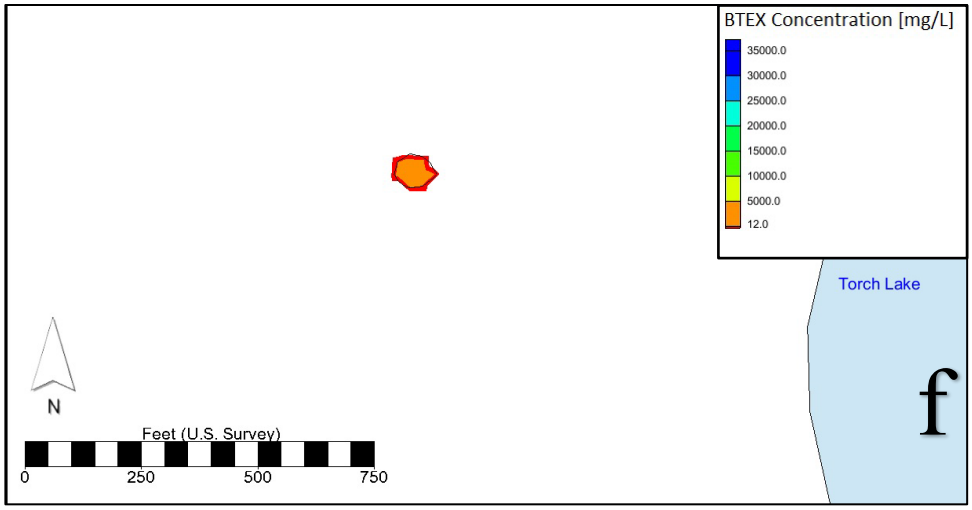

Figure 9.3: MT3DMS simulated plume extents for air injection remediation at 1 (a), 15 (b), 30 (c), 60 (d), 90 (e), and 365 (f) days. The lowest shown contour is 12 mg/L.

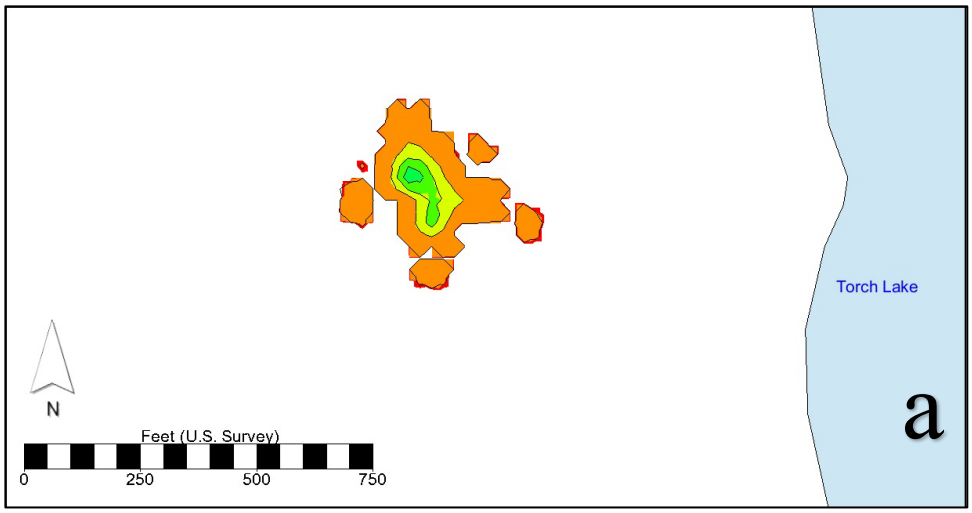

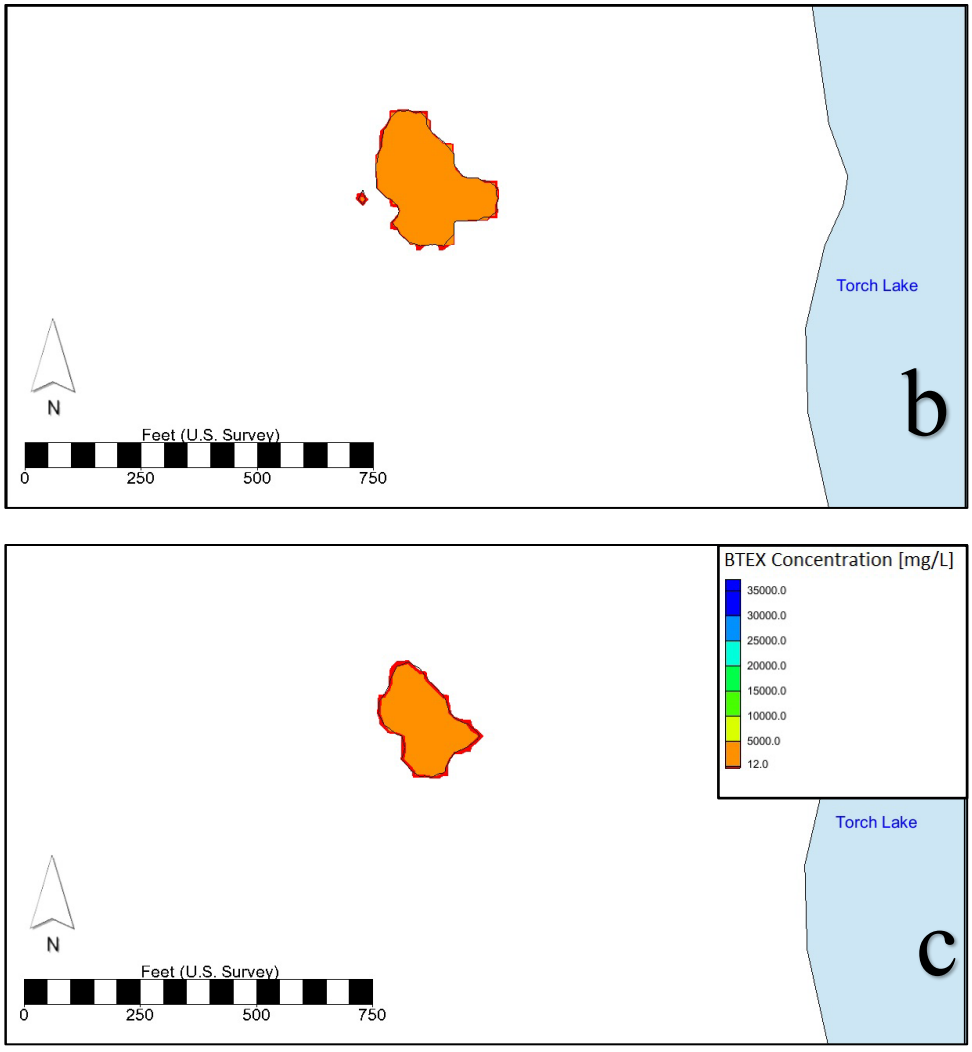

Figure 9.4: MT3DMS simulated plume extents for enhanced microbial bioremediation at 1 (a), 15 (b), and 30 (c) days. The lowest shown contour is 12 mg/L.

9.4 MODPATH Particle Tracking

The particle tracking code, MODPATH, was utilized to predict the plume travel direction with the groundwater flow. The calculated travel paths by MODPATH follow the groundwater flow velocity vectors without any dispersion nor retardation or reaction. Four particles were placed on cells that transected the BTEX plume and were tracked forward in time for five years (1,825 days). Figure 9.5 shows the visual comparison of the BTEX plume with no degradation at 1,825 days, its transport extent, and the MODPATH path lines. The MT3DMS forecast of plume movement should be centered on the calculated corresponding positions from MODPATH.

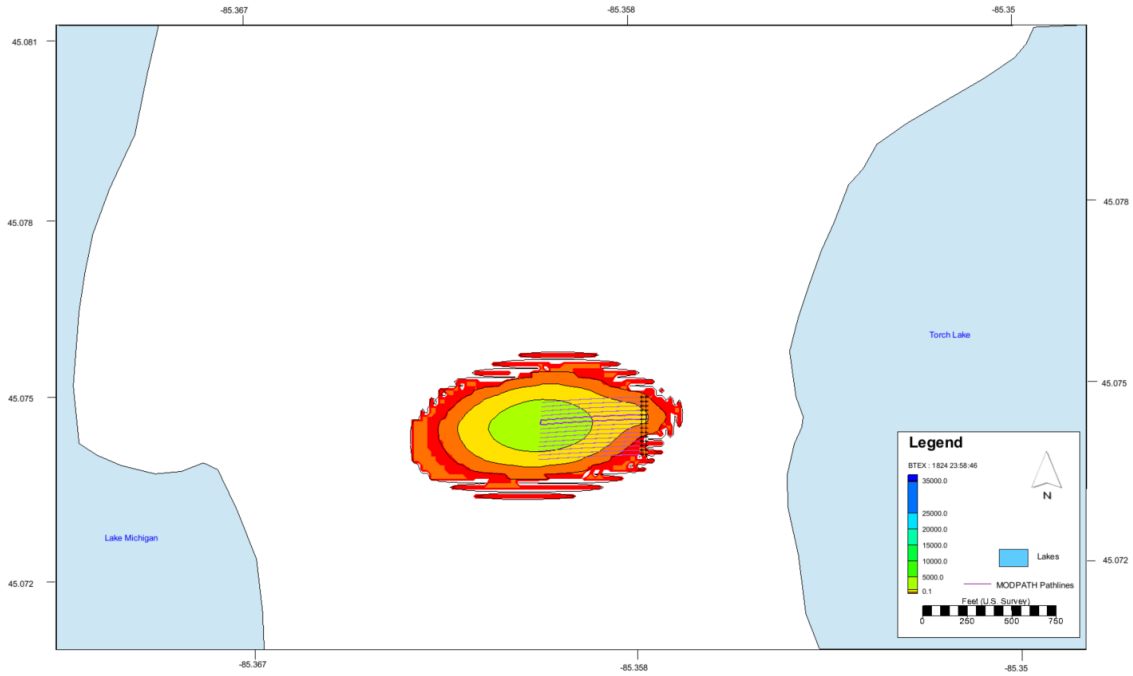

Figure 9.5: MT3DMS simulated BTEX plume with no degradation compared to MODPATH path lines tracked forward in time for five years.

10 Copyright documentation

All images in this document are either self-made or from Wikipedia. They are all public domain, or licensed for reuse under Creative Commons license 3.0. Please see below for full citation and attribution information.

Figure 2.4. "The various representations of benzene." By Vladsinger (2009) at the English language Wikipedia. Licensed under CC BY-SA3.0 via Wikimedia Commons - https://en.wikipedia.org/wiki/Benzene#/media/File:Benzene_Representations.svg. Accessed March 2022.

Figure 2.4. "Structure of Toluene." By NEUROtiker (2007) at the English language Wikipedia. Licensed under public domain via Wikimedia Commons - https://en.wikipedia.org/wiki/Toluene#/media/File:Toluol.svg. Accessed March 2022.

Figure 2.4. "Skeletal formula of the ethylbenzene molecule. Structure based on X-ray crystallographic data reported in Acta Cryst. (2013) C13, 273–276 Image generated in ChemDraw Professional 19.0 and converted into SVG file using Scribus 1.5.4 + Inkscape 1.0.1 (drawn according to official Manual of Style guidelines)." By Chem Sim 2001 (2020) at the English language Wikipedia. Licensed under public domain via Wikimedia Commons - https://en.wikipedia.org/wiki/File:Ethylbenzene-2D-skeletal.svg. Accessed March 2022.

Figure 2.4. "Chemical structures of ortho-, meta-, and para-xylenes." By Calvero (2006) at the English language Wikipedia. Licensed under public domain via Wikimedia Commons - https://upload.wikimedia.org/wikipedia/commons/e/e2/Xylenes.png. Accessed March 2022